

MOL #49783

**Full pharmacological efficacy of a novel S1P<sub>1</sub> agonist that does not require S1P-like head-group interactions**

Pedro J. Gonzalez-Cabrera<sup>†</sup>, Euijung Jo<sup>†</sup>, M. Germana Sanna<sup>†</sup>, Steven Brown<sup>†</sup>, Nora Leaf, David Marsolais, Marie-Therese Schaeffer, Jacqueline Chapman, Michael Cameron, Miguel Guerrero, Edward Roberts and Hugh Rosen

Departments of Chemical Physiology & Immunology (PJG-C, EJ, MGS, NL, DM, HR), Chemistry (MG, ER) and The Scripps Research Institute Molecular Screening Center (M-TS, JC, SB, HR), 10550 North Torrey Pines Rd, La Jolla, CA 92037

Translational Research Institute, Scripps Florida, 5353 Parkside Drive, Jupiter, FL 33458 (MC)

MOL #49783

**Running title:** S1P<sub>1</sub> agonism efficacy without headgroup interactions

**Address correspondence to:** Hugh Rosen

Phone: 858-784-2396

Fax: 858-784-2010

[hrosen@scripps.edu](mailto:hrosen@scripps.edu)

**Text pages:**

**Number of tables:** 5

**Number of figures:** 7

**References:** 33

**Footnotes:** 1

**Words in the *Abstract*:** 250

**Words in the *Introduction*:** 764

**Words in the *Discussion*:** 944

**Abbreviations:** CYM-5442, 2-(4-(5-(3,4-diethoxyphenyl)-1,2,4-oxadiazol-3-yl)-2,3-dihydro-1H-inden-1-yl amino) ethanol; SEW2871, 5-[4-phenyl-5-(trifluoromethyl)-2-thienyl]-3-[3-(trifluoromethyl) phenyl]-1, 2, 4-oxadiazole; W146, (R)-3-Amino-(3-hexylphenylamino)-4-oxobutylphosphonic acid; GTP $\gamma$ S, guanosine 5'-O-[gamma-thio]triphosphate; EDTA, ethylenediaminetetraacetic acid; MAPK, Mitogen activated protein kinase; FTY720, 2-amino-2-(4-octylphenethyl)propane-1,3-diol; CYM-5181, 5-(3,4-diethoxyphenyl)-1,2,4-oxadiazol-3-yl; AFD, 2-amino-4-(4-(heptyloxy)phenyl)-2-methylbutyl dihydrogen phosphate.

MOL #49783

## Abstract

Strong evidence exists for interactions of zwitterionic phosphate and amine groups in Sphingosine-1 phosphate (S1P) to conserved R and E residues present at the extracellular face of transmembrane-3 (TM3) of S1P receptors. The contribution of R<sup>120</sup> and E<sup>121</sup> for high affinity ligand-receptor interactions is essential, as single-point R<sup>120</sup>A or E<sup>121</sup>A S1P<sub>1</sub> mutants neither bind S1P nor transduce S1P function. Because S1P receptors are therapeutically interesting, identifying potent selective agonists with different binding modes and *in vivo* efficacy is of pharmacological importance. Here we describe a modestly water-soluble highly-selective S1P<sub>1</sub> agonist (CYM-5442) that does not require R<sup>120</sup> or E<sup>121</sup> residues for activating S1P<sub>1</sub>-dependent p42/p44 MAPK phosphorylation, which defines a new hydrophobic pocket in S1P<sub>1</sub>. CYM-5442 is a full agonist *in vitro* for S1P<sub>1</sub> internalization, phosphorylation and ubiquitination. Importantly, CYM-5442 was a full agonist for induction and maintenance of S1P<sub>1</sub>-dependent lymphopenia, decreasing B-lymphocytes by 65% and T-lymphocytes by 85% of vehicle. Induction of CYM-5442 lymphopenia was dose and time-dependent, requiring serum concentrations in the 50 nM range. *In vitro* measures of S1P<sub>1</sub> activation by CYM-5442 were non-competitively inhibited by a specific S1P<sub>1</sub> antagonist (W146), competitive for S1P, FTY720-P and SEW2871. In addition, lymphopenia by CYM-5442 was reversed by W146 administration or upon pharmacokinetic agonist clearance. Pharmacokinetics in mice also indicated that CYM-5442 partitions significantly in central nervous tissue. These data show that CYM-5442 activates S1P<sub>1</sub>-dependent pathways *in vitro* and to levels of full efficacy *in vivo* through a hydrophobic pocket, separable from the orthosteric site of S1P binding that is headgroup dependent.

## Introduction

S1P is a circulating lipid that binds to five G protein-coupled receptors (GPCRs) termed S1P<sub>1-5</sub>. S1P<sub>1</sub> selectively regulates physiological functions in the immune and cardiovascular systems, including immune cell trafficking (Goetzl and Rosen, 2005, Rosen et al., 2007) and maintaining endothelial integrity (Lee et al., 1999; Sanchez et al., 2004; Dudek et al., 2004; Sanna et al., 2006; Foss et al., 2007). Pharmacological studies with the sphingosine analog immunosuppressant prodrug, FTY720, indicated that administration of FTY720 or S1P decreased lymphocyte counts in the mouse draining lymph node, resulting in lymphopenia (Mandala et al., 2002). Moreover, FTY720 was shown to be rapidly phosphorylated, with the phosphorylated species (FTY720-P) acting as a potent agonist on S1P<sub>1,3-5</sub> subtypes. Discovery of SEW2871, a selective agonist for S1P<sub>1</sub> that replicated the lymphopenic actions of FTY720, plus development of selective S1P<sub>1</sub> antagonists with *in vivo* activity, later demonstrated that S1P<sub>1</sub> was the primary mediator of lymphocyte sequestration in secondary lymphoid organs and lymphopenia.

Mechanistic insights into S1P<sub>1</sub> mediated lymphopenia came from combining genetics, pharmacological tools and two-photon imaging (Wei et al., 2005; Sanna et al., 2006). The latter has allowed studying real-time lymphocyte dynamics in the intact lymph node, where SEW2871 infusion reduces lymphocyte egress in the medulla, while a selective S1P<sub>1</sub> antagonist (W146) fully reverses agonist actions.

In the thymus, S1P<sub>1</sub> agonism enhances late thymocyte maturation, yet inhibits subsequent thymocyte egress (Rosen et al., 2003; Alfonso et al., 2006; Weinreich and Hogquist, 2008). Consequently, S1P agonist administration reduces naïve blood CD4<sup>+</sup> and CD8<sup>+</sup> thymocytes and B-cells by nearly 90% and 70%, respectively.

## MOL #49783

Regulation of lymphocyte trafficking with S1P<sub>1</sub> agonists has opened the possibility for clinical modulation of lymphocyte dynamics, exemplified by the positive results reported in multiple sclerosis (MS) clinical trials with FTY720 (Hiestand et al., 2008). Although the mechanism of FTY720 in ameliorating MS symptoms is not clear, it may encompass multiple targets, both systemic, including S1P<sub>1</sub> mediated lymphopenia, and local, by actions on neurons (Kataoka et al., 2005; Belatoni et al., 2007; Miron et al., 2008). Recently, a report has also highlighted that vascular integrity of the brain blood barrier (BBB) likely participates on the mechanism of FTY720's efficacy in MS (Foster et al., 2008). Thus, understanding the contribution of systemic and local effects of S1P<sub>1</sub> modulation would be relevant for developing efficacious therapies for autoimmune disease.

Previous studies aimed at dissecting the S1P-S1P<sub>1</sub> binding pocket have provided strong evidence for a model of S1P ligand interaction with three charged residues on S1P<sub>1</sub> (Parrill et al., 2000; Wang et al., 2001). Two residues, R<sup>120</sup> and E<sup>121</sup>, which are present on TM3 of all S1P receptors, interact with the phosphate headgroup and the ammonium moiety of S1P, respectively. The importance of R<sup>120</sup> and E<sup>121</sup> interactions with S1P has been demonstrated by mutagenesis. Substitution of R<sup>120</sup> or E<sup>121</sup> with alanine results in total loss of [<sup>33</sup>P]-S1P binding to S1P<sub>1</sub>, and consistent with the lack of binding, neither of the TM3 mutants internalize following an S1P challenge, nor stimulate S1P-mediated [<sup>35</sup>S]-GTPγS binding. Thus, the strong zwitterionic nature of S1P requires hydrophilic headgroup interactions on S1P<sub>1</sub> TM3 RE residues to achieve high affinity binding and receptor functions.

MOL #49783

We have shown that besides S1P, other S1P<sub>1</sub> agonists including AFD-R (an FTY720-P analog), and SEW2871, also require R<sup>120</sup> and E<sup>121</sup> for full activation of intracellular pathways (Jo *et al.*, 2005). Interesting, although SEW2871 lacks structurally charged headgroups, its binding model to S1P<sub>1</sub> and activation of P42/p44 MAPK and AKT pathways is dependent on R<sup>120</sup> and E<sup>121</sup>, likely by replacing the salt-bridge polar interactions by ion-dipole interactions. SEW2871 has recently shown to make additional hydrophobic interactions deep in S1P<sub>1</sub> TM5, suggesting that it overlaps both the hydrophilic pocket and a hydrophobic pocket on S1P<sub>1</sub> (Fujiwara *et al.*, 2007).

Because the RE residues are invariant across S1P receptors, developing efficacious ligands that bind solely in deep hydrophobic pockets could provide advantages for selectivity, mechanism-based toxicity, and the ability of these molecules to potentially traverse impermeant barriers, like the BBB.

Here we report development and characterization of a potent and moderately water-soluble small molecule S1P<sub>1</sub>-agonist (CYM-5442) that does not require either of the critical RE S1P-S1P<sub>1</sub> headgroup interactions, yet, it is fully active *in vivo* for inducing lymphopenia. Importantly, CYM-5442 partitions significantly into brain tissue. Development of *in vivo*-active S1P<sub>1</sub> agonists that do not require headgroup interactions, like CYM-5442, reveal a discrete novel hydrophobic pocket on S1P<sub>1</sub> to be further explored in therapeutics.

## Materials and Methods

**Reagents.** S1P was purchased from Biomol. The selective S1P<sub>1</sub> agonist SEW2871 was purchased from Maybridge. The selective S1P<sub>1</sub> antagonist W146 was from Avanti Polar Lipids. The selective S1P<sub>2</sub> antagonist JTE-013 was from Cayman Medical Company. P<sup>32</sup>-orthophosphate was purchased from Perkin Elmer. The MEK1 inhibitor U0126 was from Calbiochem.

**Cell lines.** The generation of stable CHO-K1-S1P receptor cell clones and the conditions for CRE and NFAT reporter assays have been recently documented (Schurer *et al.*, 2008). The TANGO<sup>®</sup> S1P<sub>4</sub> and TANGO<sup>®</sup> S1P<sub>5</sub> stable cell lines were obtained from Invitrogen and assayed according to Invitrogen's protocols with 1  $\mu$ M S1P as positive control (Schurer *et al.*, 2008). HEK293 cells stably expressing human S1P<sub>1</sub> tagged with C-terminal GFP (S1P<sub>1</sub>-GFP) were a gift from Timothy Hla (U. Conn. Health Center, Farmington, CT). S1P<sub>1</sub>-GFP cells were grown as reported (Gonzalez-Cabrera *et al.*, 2007). Parental CHO-K1 cells used in transient transfection experiments were purchased from ATCC (Manassas, VA).

**Chemical synthesis of CYM-5442.** The schematic steps (i-iv) of CYM-5442 synthesis are indicated in Figure 2, and are as follows:

**i**  
**1-hydroxy-2,3-dihydro-1H-indene-4-carbonitrile.** To a stirred suspension of 1-oxo-2,3-dihydro-1H-indene-4-carbonitrile (1.0 equiv, 0.4M) and silica gel (catalytic) in ethanol at 0 °C was added NaBH<sub>4</sub> (0.33 equiv). The reaction was allowed to warm up to room temperature and stirred for 2 h. The Solvent was removed under reduced pressure and the product purified by C.C. in Hexane/EtOAc (5:5) to offer 1-hydroxy-2, 3-dihydro-1H-indene-4-carbonitrile as white solid in 80% yield. <sup>1</sup>H NMR (300 MHz, CDCl<sub>3</sub>):  $\delta$  7.62 (d,

MOL #49783

$J = 7.5$  Hz, 1H), 7.54 (d,  $J = 7.8$  Hz, 1H), 7.33 (t,  $J = 7.8$  Hz, 1H), 5.28 (t,  $J = 6.3$  Hz, 1H), 3.28-3.18 (m, 1H), 3.02-2.92 (m, 1H), 2.63-2.52 (m, 1H), 2.06-1.99 (m, 1H).

**ii**

*1,N-dihydroxy-indan-4-carboxamidine*. To a stirred suspension of hydroxylamine hydrochloride (1.1 equiv) and  $\text{Na}_2\text{CO}_3$  (1.1 equiv) in ethanol was added, in one portion, the benzonitrile prepared in previous step (1 equiv). The mixture was refluxed for 6 h followed by addition of another portion of hydroxylamine hydrochloride (1.1 equiv) and  $\text{Na}_2\text{CO}_3$  (1.1 equiv), the reaction was refluxed for additional 6 h. The suspension was cooled to room temperature and filtered. The solid was washed with ethanol and the filtrate was concentrated under reduced pressure. The amidoxime-crude was recrystallized from EtOAc/Hexanes and used without further purification.

**iii**

*4-[5-(3,4-Diethoxy-phenyl)-[1,2,4]oxadiazol-3-yl]-indan-1-ol*. In a microwave vial, a stirring solution of 3, 4-diethoxybenzoic acid (1 equiv, 0.2M) in DMF was treated with HOBt (1.3 equiv) and EDCI (1.3 equiv) at room temperature. The reaction was stirred for 20 min followed by addition, in a single portion, of amidoxime (prepared in previous step) (1.1 equiv). The reaction was stirred for additional 30 min at room temperature and then heated to 130 °C for 30 min. The reaction was diluted using a saturated solution of NaCl and extracted with EtOAc (X3). The organic phase was dried over  $\text{Na}_2\text{SO}_4$  anhydrous and concentrated under reduced pressure. The product was purified by C.C. using  $\text{CH}_2\text{Cl}_2$ :MeOH (9:1) to offer diaryloxadiazole as white solid in good yield.

$^1\text{H}$  NMR (400 MHz,  $\text{CDCl}_3$ ):  $\delta$  8.10 (d,  $J = 7.6$ , 1H), 7.78 (dd,  $J_1 = 1.6$  Hz,  $J_2 = 8$  Hz, 1H), 7.67 (d,  $J = 1.6$  Hz, 1H), 7.56 (d,  $J = 7.6$  Hz, 1H), 7.39 (t,  $J = 7.6$  Hz, 1H), 6.97 (d,  $J = 8.0$  Hz, 1H), 5.29 (t,  $J = 6.4$  Hz, 1H), 4.19 (q,  $J = 7.2$  Hz, 2H), 4.18 (q,  $J = 7.2$  Hz, 2H),



MOL #49783

3.51-4.43 (m, 1H), 3.22-3.14 (m, 1H), 2.59-2.51 (m, 1H), 2.04-1.97 (m, 1H), 1.5 (t,  $J = 7.2$  Hz, 3H), 1.49 (t,  $J = 7.2$ , 3H);  $^{13}\text{C}$  NMR (100 MHz,  $\text{CDCl}_3$ ):  $\delta$  175.2, 168.9, 152.8, 148.9, 146.6, 143.3, 128.9, 127.4, 127.0, 123.8, 122.2, 116.7, 112.7, 112.4, 76.2, 64.9, 64.8, 35.7, 31.5, 14.9, 14.8. MS (EI)  $m/z$  367 ( $\text{M}^+$ ), HRMS (EI) for  $\text{C}_{21}\text{H}_{22}\text{N}_2\text{O}_4$  ( $\text{M}^+$ ): calcd 367.1652, found 367.1653.

**iv**

*2-{4-[5-(3,4-Diethoxy-phenyl)-[1,2,4]oxadiazol-3-yl]-indan-1-ylamino}-ethanol (1).*

A solution of alcohol (1 equiv), at 0 °C, was treated with  $\text{SOCl}_2$  (1.1 equiv) and pyridine (1.1 equiv) in  $\text{CH}_2\text{Cl}_2$ . The reaction was stirred at room temperature for 2h. The reaction was diluted with  $\text{CH}_2\text{Cl}_2$  and washed with  $\text{NaHCO}_3$  (2X). The organic phase was dried over sodium sulfate and concentrated under reduced pressure. The crude was dissolved in DMF and treated with the ethanolamine (2 equiv) and DIPEA (2.0 equiv). The reaction was stirred at 50 °C for 48h. The reaction was diluted with  $\text{H}_2\text{O}$  and the product extracted with EtOAc (3X). The product was purified by C.C. using  $\text{CH}_2\text{Cl}_2/\text{MeOH}$  (9:1) to offer aminoethanol CYM-5442 as white solid in 60% yield.

$^1\text{H}$  NMR (500 MHz,  $\text{CDCl}_3$ ):  $\delta$  8.12 (d,  $J = 7.5$  Hz, 1H), 7.79 (dd,  $J_1 = 2.0$  Hz  $J_2 = 8.5$  Hz, 1H), 7.68 (d,  $J = 2.0$  Hz, 1H), 7.63 (d,  $J = 7.5$  Hz, 1H), 7.40-7.37 (m, 1H), 4.49-4.47 (m, 1H), 4.23-4.16 (m, 4H), 3.78-3.70 (m, 1H), 3.53-3.46 (m, 1H), 3.29-3.22 (m, 1H), 2.96-2.94 (m, 4H), 2.56-2.50 (m, 1H), 2.09-2.03 (m, 1H), 1.52-1.49 (m, 6H);  $^{13}\text{C}$  NMR (125 MHz,  $\text{CDCl}_3$ ):  $\delta$  175.03, 168.66, 152.71, 148.87, 143.76, 128.71, 127.11, 123.89, 122.04, 116.67, 112.63, 112.49, 104.66, 64.84, 64.61, 62.70, 60.34, 47.98, 31.90, 29.69, 14.72, 14.64. MS (EI)  $m/z$  410 ( $\text{M}^+$ ), HRMS (EI) for  $\text{C}_{23}\text{H}_{27}\text{N}_3\text{O}_4$  ( $\text{M}^+$ ): calcd 410.2074, found 410.2077.

**Evaluation of CYM-5442 agonist properties.** Details of the screening CRE reporter assays can be found in Schurer et al., (2008). For the CRE reporter assay studies, forskolin was included at a 2  $\mu$ M final concentration prior to addition of the agonists. Agonist-mediated inhibition of forskolin induced cAMP accumulation was read on an Envision fluorescent plate reader (384-well format) after 2 h agonist incubation, and with SEW2871 as the positive control. Agonist-induced S1P<sub>1</sub>-GFP internalization and ubiquitination assays have been documented previously (Gonzalez-Cabrera et al., 2008). Description of agonist-mediated S1P<sub>1</sub>-GFP phosphorylation experiments can be found in Schurer et al., (2008).

**ELISA determination of p42/p44 MAPK activity.** CYM-5442 and S1P-mediated p42/p44 MAPK activation was measured using an ELISA kit (Cell Signaling Technologies) in CHO-K1 cells transiently transfected with either the WT S1P<sub>1</sub> receptor cDNA or the single-point S1P<sub>1</sub> mutant (R<sup>120</sup>A or E<sup>121</sup>A) cDNAs (gifts from Abby Parrill, University of Memphis, TN). For transfections, cells were plated on 10-cm dishes at 80% confluence and transfected with 12  $\mu$ g of each plasmid using Fugene HD (Roche) in Opti-MEM. After 16 h, each pool transfected dish was split into a 6-well plate and allowed to incubate for additional 24 h. The cells were next incubated for 4 h in serum-free DMEM prior to addition of the agonist. In the antagonist (W146) experiments or the MEK1 inhibitor (U0126), W146 or U0126 were incubated for 30 min (U0126) or 1 h (W146) at 10  $\mu$ M prior to agonist treatment. Cells were then stimulated for 5 min (determined empirically to be maximal for both agonists) with increasing concentrations of CYM-5442 or S1P and activation of p42/p44 MAPK phosphorylation was assayed according to manufacturer instructions. For each condition (WT, R<sup>120</sup>A or E<sup>121</sup>A), both

## MOL #49783

CYM-5442 and S1P agonists were tested in parallel, in presence and absence of W146. In addition, for each of the conditions tested, the concentration response curves for agonist-mediated activation of p42/p44 MAPK phosphorylation were plotted as a percent of the agonist eliciting the maximal response, and the potency (EC<sub>50</sub>), maximal response (E<sub>max</sub>) and goodness of fit (R<sup>2</sup>) values were determined using Graph Pad Prism (San Diego, CA).

**Pharmacokinetic studies.** Pharmacokinetics of CYM-5442 was assessed in Sprague Dawley rats. The compound was formulated at 1 mg/ml (10:10:80, DMSO: tween 80: water, vol:vol:vol) and dosed at 1 mg/kg intravenous (i.v.) into the jugular or 2 mg/kg by oral gavage (P.O.). Blood was obtained at t= 5 min, 15 min, 30 min, 1 h, 2 h, 4 h, 6 h, and 8 h into EDTA containing tubes and plasma was generated by standard centrifugation methods. Separate studies to evaluate brain exposure were done in C57Bl6 mice where CYM-5442 was dosed at 10 mg/kg by intraperitoneal (i.p.) route. Blood and brains were obtained at t= 2 h to assess the amount of compound in the target organ. All procedures and handling were according to standard operating procedures approved by the Institutional Animal Care and Use Committee (IACUC).

In order to assess *in vivo* pharmacokinetic parameters an LC-MS/MS bioanalytical method was developed where 25 µl of plasma was treated with 125 µl of acetonitrile containing an internal standard in a Millipore Multiscreen Solvinter 0.45 micron low binding PTFE hydrophilic filter plate (#MSRLN0450) and allowed to shake at room temperature for five minutes. The plate was then centrifuged for 5 minutes at 4,000 rpm in a tabletop centrifuge and the filtrate was collected in a polypropylene capture plate. The filtrate (10 µl) was injected using an Agilent 1200 HPLC equipped

## MOL #49783

with a Thermo Betasil C18 HPLC column 5  $\mu$  (50 x 2.1 mm; # 70105-052130). Mobile Phase A was water with 0.1% formic acid. Mobile Phase B was acetonitrile with 0.1% formic acid. Flow rate was 375  $\mu$ l/min using a gradient of 90% A/10% B from 0-0.5 min,, ramped to 5%A/95%B at 2 min, held at 5%A/95%B until 3.0 min, ramped to 90% A/10% B at 4 min, and held at 90% A/10% B until 7 min. An API Sciex 4000 equipped with a turbo ion spray source was used for all analytical measurements. Instrument settings had curtain gas set to 10, gas 1 and gas 2 set to 45, ionization energy set to 5500 Volts, drying gas temperature 550°C, resolution was set to unit, and dwell time was set to 100 msec. A positive ion MRM method was developed. CYM-5442 was quantitated from 2 to 1000 ng/mL. Peak areas of the  $m/z^0 410.1 \rightarrow 193.1$  product ion of CYM-5442 (DP = 45, CE = 30) were measured against the peak areas of the internal standard (sunitinib)  $m/z$  399 $\rightarrow$ 283 product ion (DP = 86, CE = 41). Data was fit using WinNonLin (Pharsight Corporation, Mountain View, CA).

Similar conditions were used to determine brain levels of CYM-5442 except the brain samples were frozen upon collection. When analyzed the frozen samples were weighed and acetonitrile was added (10x weight: vol). The samples were sonicated to extract the compound from the brain matrix and then filtered as described above. Brain samples were analyzed against a standard curve generated in blank brain matrix.

**Measurement of CYM-5442 mediated lymphopenia.** Male C57BL6 mice weighing 30 g were used for all experiments. All animal studies were approved by the IACUC. Animals were injected i.p. with a volume of 300  $\mu$ l with the indicated dose of CYM-5442 or vehicle. For W146 experiments, mice were administered with 20 mg/kg W146 or vehicle for 30 min prior to CYM-5442 administration. Vehicle consisted of

## MOL #49783

sterile water (CYM-5442) or 10% DMSO, 25% Tween-20 in sterile water (W146).

Following incubation at the indicated times, animals were euthanized and blood collected into tubes containing EDTA. Blood white blood cell count and lymphocyte counts were obtained using an automated veterinary Hemoanalyzer (Hospitex Diagnostics, TX) by reading 30  $\mu$ l blood samples. The remaining blood was used for determination of drug serum levels (see below), or to determine, by FACs, the number of B-cells (using a FITC conjugated B220 antibody marker, BD Diagnostics, 1:100 dilution) and T-cells (using Pacific Blue CD4<sup>+</sup> and Per-CP-Cy5.5 CD8<sup>+</sup> antibodies; BD Diagnostics, both at 1:100). FACS analysis was done in FlowJo (Ashland, OR).

**CYM-5442 and W146 serum concentration.** Blood samples used in lymphopenia studies were further processed for measuring serum CYM-5442 and W146 concentrations. Samples (100  $\mu$ l plasma) were extracted with 400  $\mu$ l ice cold methanol (stored at -20°C), vortexed for 1 min, allowed to sit at 4°C for 30 min, and centrifuged at 16,400 rpm for 5 min. The supernatant was evaporated to a volume near dryness and methanol was added to bring the final volume to 50  $\mu$ l. For calibration standards, clean plasma was spiked with increasing concentrations of CYM-5442 or W146, and processed the same way as the samples. Samples were analyzed on an Agilent LC-MS/MS system using an 1100 LC stack mated with a 6410 triple quadrupole mass spectrometer. For CYM-5442 quantification, the transition of m/z 410  $\rightarrow$  349.2 was monitored, and for W146, the transition of m/z 343  $\rightarrow$  138 was monitored. The column used was an Agilent Zorbax SB-C18 (2.1 mm x 75 mm). Flow-rate = 250 ml per min. Mobile phases were A = water: 0.1% formic acid, B = acetonitrile: 0.1% formic acid. Gradient: T=0, 15% B - >T = 8, 98% B; 5  $\mu$ l injected.

## Results

**CYM-5442 is a potent S1P<sub>1</sub> selective agonist.** CYM-5442 (Figure 1) is a chemically optimized version of an original hit (CYM-5181) from a screen aimed to discover novel S1P receptor agonists (Schurer et al., 2008). The chemical synthesis of CYM-5442 is depicted in Figure 2. Even though CYM-5442 contains the privileged oxadiazole-based scaffold reported to fit S1P receptors (Schurer et al., 2008), CYM-5442 is selective for S1P<sub>1</sub>, as measured by high throughput agonist-antagonist formats across S1P receptors (Table 1). In high throughput agonist format with SEW2871 as the positive control, CYM-5442 inhibited forskolin-stimulated CRE transcription in a concentration dependent manner (Figure 3), being a full agonist compared to SEW2871, but of higher potency (20-fold and 100-fold) relative to CYM-5181 and SEW2871, respectively.

Further characterization of the agonist properties of CYM-5442 was done using a receptor immunoprecipitation protocol previously validated for studying trafficking and fate of S1P<sub>1</sub>-GFP during agonist stimulation (Gonzalez-Cabrera et al., 2007). Using this protocol and HEK293 cells stably expressing S1P<sub>1</sub> fused to GFP on the carboxy-terminus, we probed CYM-5442 for stimulating three agonist-S1P<sub>1</sub> activated steps: receptor phosphorylation, receptor internalization and receptor-ubiquitin recruitment. Figure 4A indicates that incubation of 500 nM CYM-5442 with P<sup>32</sup>-orthophosphate labeled cells stimulated S1P<sub>1</sub> phosphorylation in a time-dependent manner, similar to that obtained with 500 nM of S1P (at 30 min). CYM-5442 led to rapid S1P<sub>1</sub> phosphorylation which was sustained throughout the analysis. To confirm the involvement of S1P<sub>1</sub> for CYM-5442 phosphorylation, the S1P<sub>1</sub> selective antagonist W146 was used. Pre-incubation

MOL #49783

with 10  $\mu$ M of W146 for 30 min prior to CYM-5442 treatment completely abolished CYM-5442-mediated S1P<sub>1</sub> phosphorylation, while antagonist alone had no effect on the response. In addition, silver staining of the same gel used to measure receptor phosphorylation indicated that the differences in S1P<sub>1</sub> phosphorylation across conditions were not due to differences in immunoprecipitated S1P<sub>1</sub> protein loading.

Membrane-associated GPCRs are usually internalized into cytosolic vesicles upon agonist stimulation. We and others have shown that S1P and S1P agonist analogs internalize S1P<sub>1</sub>-GFP from the plasma membrane to cytoplasmic vesicles (Liu et al., 1999; Gonzalez-Cabrera et al., 2007; Oo et al., 2007). Figure 4B shows that incubation of S1P<sub>1</sub>-GFP cells with 500 nM CYM-5442 stimulated the internalization of S1P<sub>1</sub>-GFP receptor from a membrane-associated localization to an intracellular, multivesicular compartment. Similar internalization pattern was obtained by 0.5  $\mu$ M S1P incubation (not shown). Internalization of S1P<sub>1</sub>-GFP by CYM-5442 was completely blocked by preincubation with 10  $\mu$ M W146, and consistent with the phosphorylation data, W146 alone did not have an effect on internalization.

S1P<sub>1</sub> agonism with some ligands, termed supraphysiological because of their ability to alter receptor signaling reserve, results in degradation of S1P<sub>1</sub>-GFP in lysosomes and proteasomes, and the magnitude of agonist-dependent receptor ubiquitination has been reported to influence receptor fate (Gonzalez-Cabrera et al, 2007; Oo et al, 2007). Thus, agonist recruitment of ubiquitin to S1P<sub>1</sub> can be used as a measure of ligand receptor activation. The ability of AFD-R, a highly efficient ubiquitinase (Gonzalez-Cabrera et al, 2007; Oo et al, 2007), and CYM-5442 to recruit ubiquitin onto immunoprecipitated S1P<sub>1</sub>-GFP is shown in Figure 4C. CYM-5442 stimulated receptor

MOL #49783

ubiquitination (UB-S1P<sub>1</sub>-GFP) to AFD-R levels. Ubiquitination by the agonists resulted in high mass-weight smears (approximately from 97 KDa to 180 KDa) of ubiquitin-receptor complexes running immediately above the immunoprecipitated receptor. Pre-incubation with the selective antagonist W146 was shown to nearly abolish CYM-5442-stimulated S1P<sub>1</sub> ubiquitination. Overall, the *in vitro* data indicates that CYM-5442 is a potent and selective S1P<sub>1</sub> agonist.

**CYM-5442 does not require ionic S1P-receptor headgroup interactions for activating S1P<sub>1</sub>-mediated p42/p44 MAPK phosphorylation.** S1P and synthetic S1P<sub>1</sub> agonists have been shown to activate the mitogenic p42/p44-MAPK pathway across many cell types (Sorensen et al., 2003; Jo et al., 2005; Ahmad et al., 2006). The ability of CYM-5442 and S1P to activate p42/p44-MAPK was studied by ELISA, using lysates of CHO-K1 cells transiently expressing either the human wild-type S1P<sub>1</sub> (WT) or the two separate single-point S1P<sub>1</sub> mutants (R<sup>120</sup>A and E<sup>121</sup>A), known to abolish binding and activity of S1P on S1P<sub>1</sub>. Time-course studies demonstrated that maximal p42/p44-MAPK activity was achieved at 5 minutes in CHO-K1 cells expressing S1P<sub>1</sub> (Supplemental Figure 1A). The time-course also showed that treatment with 500 nM S1P for 5 min did not lead to measurable p42/p44 MAPK activity in mock-transfected CHO-K1 cells. S1P and CYM-5442 stimulated P42/P44 MAPK phosphorylation was completely blocked by pre-incubation with 10  $\mu$ M of the MEK1 inhibitor U0126 (Supplemental Figure 1B).

Using the 5 min incubation time, we sought to determine the requirement of S1P<sub>1</sub> R<sup>120</sup> and E<sup>121</sup> residues for CYM-5442 and/or S1P activation of P42/P44 MAPK. For these experiments, concentration response curves with the agonists were performed on



# MOL #49783

cells expressing each of the single point mutants ( $R^{120}A$  and  $E^{121}A$ ), and these responses were compared to those in the WT receptor, both in the presence and absence of the selective  $S1P_1$  antagonist W146. Figure 5 shows the plots of the average concentration responses in the three transfectants, while the potency ( $EC_{50}$ ), maximal response ( $E_{max}$ ) and goodness of fit ( $R^2$ ) value estimates derived from curve fitting are included in Table 2. In WT cells, both S1P and CYM-5442 led to the concentration dependent activation of P42/P44 MAPK phosphorylation, with  $EC_{50}$  values of 2.3 nM and 46 nM, respectively. In WT transiently transfected CHO-K1 cells, S1P was a full agonist ( $E_{max}$  of 1.0 or 100%) while CYM-5442 was a partial agonist ( $E_{max}$  of 0.7 or 70% of S1P). Incubation of 10  $\mu M$  W146 prior to addition of S1P resulted in a significant rightward shift (60-fold,  $EC_{50}$  of 140 nM) in potency of S1P vs. S1P alone (Figure 5). On the other hand, preincubation with W146 in WT cells led to the complete inhibition of CYM-5442-mediated p42/p44 MAPK phosphorylation (Figure 5). These results indicate that W146 is a competitive antagonist with S1P and a non-competitive antagonist against CYM-5442.

As expected, substitution of  $S1P_1$   $R^{120}$  for alanine ( $R^{120}A$ ) resulted in a near loss of p42/p44 MAPK activity for S1P. Curve fitting the S1P data in this mutant indicated relatively poor fits ( $R^2 < 0.4$ ). Interestingly, the  $R^{120}A$  mutant was still able to maintain p42/p44 MAPK activity when incubated with CYM-5442, and as a result, the data was plotted relative to CYM-5442 maximum. The  $EC_{50}$  for CYM-5442 in the  $R^{120}A$  mutant was determined to be not-significantly different to that of WT CYM-5442 cells ( $R^{120}A$   $EC_{50}$ , 67 nM; WT  $EC_{50}$ , 46 nM). Unlike WT cells, preincubation of 10  $\mu M$  W146 in mutant  $R^{120}A$  cells did not significantly alter the p42/p44 MAPK activity by CYM-5442,

MOL #49783

and led to a modest (3-fold) rightward shift in EC<sub>50</sub> (67 nM), suggesting that in the absence of headgroup localization, W146 is a weak competitive antagonist of the hydrophobic site.

Consistent with the notion that S1P makes a functional headgroup interaction with E<sup>121</sup>, S1P did not lead to significant p42/p44 MAPK activation in E<sup>121</sup>A S1P<sub>1</sub> mutant cells. On the other hand, activation of p42/p44 MAPK by CYM-5442 in E<sup>121</sup>A S1P<sub>1</sub> cells was concentration dependent, with a mean EC<sub>50</sub> value of 134 nM. W146 preincubation led to a 10-fold rightward shift in potency of CYM-5442 for activating p42/p44 MAPK phosphorylation in E<sup>121</sup>A transfected cells. These results indicate that for S1P<sub>1</sub> dependent p42/p44 MAPK activation, CYM-5442 does not require the R<sup>120</sup> and E<sup>121</sup> S1P<sub>1</sub> residues that make up functional S1P-S1P<sub>1</sub> headgroup interactions.

**CYM-5442 pharmacokinetics.** We next evaluated the pharmacokinetics of CYM-5442 in rats. Measures included are depicted in Table 3. Overall, CYM-5442 was modestly orally bioavailable (F=26%). Routes of delivery influenced the half-lives (t<sub>1/2</sub>) of 50 min. (i.v.) and 3 h (P.O.), which supported its use *in vivo*. Notably, in mice, CYM-5442 administration was highly central nervous system penetrant. An i.p. dose of 10 mg/kg for 2 h resulted in a 13.7 ± 2.9 μM concentrations in brain compared to 1.08 ± 0.3 μM in plasma. This brain to plasma ratio of approximately 13:1 suggests that CYM-5442 may be a useful tool for studying the roles of S1P<sub>1</sub> in the central nervous system.

**CYM-5442 induces and maintains lymphopenia in mice through S1P<sub>1</sub> activation.** Administration of S1P<sub>1</sub> agonists like SEW2871 or FTY720-P induces rapid and reversible lymphopenia in mice (Mandala et al., 2002, Sanna et al., 2004). To determine whether CYM-5442 could lead to the induction of lymphopenia, we treated

MOL #49783

mice i.p. with a dose of 10 mg/kg and compared whole blood white blood cell (WBC) count and the number of circulating B-cells and T-cells, against vehicle treated mice. A five hour treatment protocol was chosen based on the pharmacokinetic data (Table 3). WBC counts in CYM-5442 animals were decreased by 64 % vs. vehicle at 5 h (Table 4). FACS analyses of whole blood from treated animals indicated that CYM-5442 decreased B220<sup>+</sup> B-cells by 63% compared to vehicle, whereas CD4<sup>+</sup> and CD8<sup>+</sup> T-cell counts were decreased by 83% and 84% of vehicle, respectively. This data indicates that a single dose of CYM-5442 induces acute lymphopenia in mice.

To ascertain whether the effects of CYM-5442 were dose-dependent, we employed a 5 h treatment and a dosing range of 0.3-10 mg/kg. The dose-response of CYM-5442 for inhibiting CD4<sup>+</sup> and CD8<sup>+</sup> cell populations is shown in Figure 6A, and a representative example of the FACS scatter plots in individual mice is shown in Figure 6B. The data indicates that CYM-5442 decreased CD4<sup>+</sup> and CD8<sup>+</sup> cell counts in a dose-dependent manner, attaining near-maximal effects on inhibition of these cell populations at serum CYM-5442 levels that ranged between 50 nM to 100 nM. Overall, the CYM-5442 mediated inhibition of B-cell and T-cell number had an estimated ED<sub>50</sub> of 0.5, 2.0 and 1.0 mg/kg for CD4<sup>+</sup>, CD8<sup>+</sup> and B220<sup>+</sup>, respectively (Figure 6C).

Next, we measured the time-course for CYM-5442 mediated lymphopenia, and whether CYM-5442 effects could be reversed upon agonist clearance from plasma. These studies were performed employing a 16 h window, and both B-cell and T-cell counts were determined in conjunction with measures of serum CYM-5442 drug levels from the same animals (Figure 6D). A representative example of individual animal FACS scatter plots is shown in Figure 6E. With a fixed dose of 10 mg/kg, shown in

MOL #49783

Figure 5A to be maximal for CYM-5442 induction of B-cell and T-cell lymphopenia, the data indicates that CYM-5442 CD4<sup>+</sup> and CD8<sup>+</sup> counts dropped significantly during the first 3 h of administration, and appeared to be maintained at these low levels from 3 h to 5 h. After five hours, the B-cell and T-cell counts began to reverse towards basal levels; consistent with the time in which CYM-5442 began to disappear from plasma.

Consistent with the dose-response data on Figure 5A, CYM-5442 induction and maintenance of lymphopenia in the time-course study occurred at serum levels of CYM-5442 ranging between 50-100 nM. The direct relationship between B-cell and T-cell recovery and loss of plasma serum CYM-5442 content thus suggested that CYM-5442 mediated lymphopenia can be reversed upon CYM-5442 clearance from the organism.

The minimal signal for lymphocyte sequestration and induction of lymphopenia by S1P<sub>1</sub> agonists depends on activation of S1P<sub>1</sub>. To ascertain whether the *in vivo* effects of CYM-5442 were due to S1P<sub>1</sub> receptor activation, we used the selective S1P<sub>1</sub> antagonist, W146, shown here to block all of the measures of CYM-5442 activation *in vitro*. For antagonist studies, we used a 5 h window and a dose of CYM-5442 of 2 mg/kg, which is close to the ED<sub>50</sub> for CYM-5442 induction of B-cell and T-cell lymphopenia (Figures 6A and 6C). A competing dose of W146 of 20 mg/kg was first administered to mice and allowed to equilibrate for 30 min prior to CYM-5442 administration. Table 5 shows that at near ED<sub>50</sub>, CYM-5442 led to the reduction of CD4<sup>+</sup>, CD8<sup>+</sup> and B220<sup>+</sup> cell counts by approximately 50% of vehicle, while W146 was able to partially recover CYM-5442 effects on B-220<sup>+</sup>, CD4<sup>+</sup> and CD8<sup>+</sup> cell counts. Importantly, neither administration of W146 alone nor of vehicle had measurable effects on cell counts (data

MOL #49783

not shown). This indicates that CYM-5442 mediated lymphopenia is dependent on S1P<sub>1</sub> receptor activation.

## Discussion

Using a chemical approach, we have characterized a small molecule compound, CYM-5442, as a selective and efficacious S1P<sub>1</sub> agonist for inducing and maintaining lymphopenia *in vivo*. It is of interest that the pharmacological properties of CYM-5442 for activating S1P<sub>1</sub>-dependent pathways are distinct from S1P, in that the ligand has no groups capable of mimicking the head-groups of S1P. The data strongly suggest that CYM-5442 interacts with S1P<sub>1</sub> in a binding pocket separate from key S1P<sub>1</sub> residues R<sup>120</sup> and E<sup>121</sup> essential for high affinity S1P binding and receptor activation (Parrill et al., 2000; Wang et al., 2001; Jo et al., 2005). Alternative residues of the putative hydrophobic pocket interacting with oxadiazole series of compounds, such as the original S1P<sub>1</sub> agonist screening hit CYM-5181, have been recently published by Schurer et al., (2008). Because CYM-5442 has an EC<sub>50</sub> within a factor of 3 of CYM-5181, the binding free energies are within experimental error of each other, and thus the docking of the ligand CYM-5442 into the receptor pocket is the same as the model shown for CYM-5181 (Figures 6, Schurer et al, (2008)) and distinct from the head-group constrained interactions of S1P (Supplementary Figure 5, Schurer et al (2008)). These differences between S1P and CYM-5442 find expression quantitatively by the retention of CYM-5442 activation of the E<sup>121</sup>A and R<sup>120</sup>A receptor mutants which fail to respond to S1P, as well as by the different mode of inhibition for CYM-5442 compared to S1P using the S1P<sub>1</sub> antagonist W146. Mutagenesis of either R<sup>120</sup> or E<sup>121</sup> residues, present on the extracellular face of TM3, to alanine, has been shown to abolish S1P-S1P<sub>1</sub> binding and subsequent receptor activation (Parrill et al., 2000; Wang et al., 2001; Jo et al., 2005), due to the inability of the charged phosphate and ammonium headgroups in S1P to make

MOL #49783

polar interactions with neutral alanine on the R<sup>120</sup>A and E<sup>121</sup>A mutants. While S1P stimulated MEK1 dependent p42/p44 MAPK phosphorylation in WT cells in a concentration-dependent manner, and with a potency consistent with literature values (Mandala et al., 2002; Sanna et al., 2004), neither of the mutant receptors was able to elicit significant signal when treated with S1P. On the other hand, the same single-point mutants, shown to be unresponsive to S1P, were still able to fully activate MEK1-dependent p42/p44 MAPK activity when treated with CYM-5442, with potency values found to be not significantly different between WT and R<sup>120</sup>A receptors, although the E<sup>121</sup>A receptors displayed slightly lower potency than WT. These data are consistent with different receptor binding requirements for the amphiphilic orthosteric agonist, S1P, and the hydrophobic selective agonist, CYM-5442.

W146 has proved to be a reliable chiral-selective S1P<sub>1</sub> antagonist *in vitro* and *in vivo* (Yoon et al., 2008; Gonzalez-Cabrera et al., 2007; Sanna et al., 2006). As mentioned above, W146 antagonism of p42/p44 MAPK activity in these studies revealed two modes of action, competitive for S1P and non-competitive for CYM-5442. W146 antagonism of S1P<sub>1</sub> signaling is therefore independent of whether S1P<sub>1</sub> activation is occurring through the orthosteric site or an adjacent hydrophobic site. Evidence for the spatial proximity of the orthosteric pocket to the hydrophobic one is provided by the competitive antagonist shift of W146 in the R<sup>120</sup>A or E<sup>121</sup>A mutated receptors in response to activation by CYM-5442. Since W146 is an amino-phosphonate, capable of making RE headgroup interactions, these data suggest that W146 is no longer constrained in the single point mutants thus allowing more flexible binding within the hydrophobic pocket. Consistent with these data, non-competitive inhibition of CYM-5442 function was also observed

MOL #49783

with W146 in U2OS cells coupled to TANGO<sup>®</sup> S1P<sub>1</sub>-bla, while W146 in the same assay was a competitive inhibitor against S1P (not shown). Other S1P<sub>1</sub> selective agonists with similar structures to CYM-5442 also display non-competitive W146 inhibition (not shown), suggesting that diaryl-oxadiazole agonists like CYM-5442 interact with a common hydrophobic pocket on S1P<sub>1</sub> (Schurer et al., 2008).

The *in vivo* data with CYM-5442 demonstrates its usefulness for inducing and maintaining S1P<sub>1</sub>-dependent lymphopenia, with a minimal serum concentration for achieving maximal lymphopenia around 50 nM. Since systemic S1P<sub>1</sub> antagonism with W146 reversed CYM-5442-induced lymphopenia, and W146 alone had no effect on B-cell and T-cell counts, the data indicates that S1P<sub>1</sub> agonist signals are minimal and obligatory for lymphopenia induction. These data provide additional evidence against the functional antagonism hypothesis for S1P<sub>1</sub>-mediated immunomodulation (Matloubian et al., 2004; Schwab and Cyster, 2007).

All effects of CYM-5442 both *in vitro* and *in vivo* are reversed or abolished by the selective S1P<sub>1</sub> receptor antagonist W146. These data restrict the pharmacological effects of CYM-5442 to this single receptor subtype. Though CYM-5442 is an enantiomeric mixture of 2 isomers, this mixture does not appear to contribute to the pharmacology or selectivity based upon our selective antagonist studies. Work is still ongoing to resolve the enantiomers. Differential crystallization using chiral salt forms such as L-tartaric acid have thus far been unsuccessful. Separation using chiral columns by HPLC is currently ongoing with no positive results yet and an enantio-specific synthesis may be formally required.



MOL #49783

CYM-5442 possesses additional properties that make it a useful S1P<sub>1</sub> chemical agonist. CYM-5442 was found to be 10,000-fold selective for S1P<sub>1</sub> over S1P<sub>5</sub>. Besides selectivity, CYM-5442 is approximately 10-50-fold more potent than SEW2871 *in vitro*, depending on which agonist format was used, and induces lymphopenia at approximately 5 to 10-fold lower doses than SEW2871. Favorable pharmacokinetics and moderate water solubility would make CYM-5442 a useful tool for studying S1P<sub>1</sub> function in tissues where drug formulation or penetrance may present challenges (i.e., lung and central nervous system). The levels of CYM-5442 in brain tissue, with a brain-plasma ratio of 13:1 following a bolus dose in mice, are notable. The beneficial effects of FTY720 in ameliorating MS symptoms have been associated, in part, with the inhibition of BBB leakiness occurring during disease progression. CNS-penetrant and efficacious non-prodrug S1P<sub>1</sub> agonists such as CYM-5442, that are also antagonist reversible in the periphery, may be good proof-of-concept chemical tools for investigating the contributions of S1P<sub>1</sub> to MS therapy. These allow the contributions of BBB integrity, lymphocyte sequestration and glial and neuronal S1P<sub>1</sub> function to be assessed. Certainly, selective S1P<sub>1</sub> agonists and antagonists have shown to inversely modulate the integrity of endothelial barriers *in vivo* (Sanna et al., 2006; Foss et al., 2007). We have data indicating that endothelial integrity is tonically regulated by the S1P-S1P<sub>1</sub> axis (Sanna et al., 2006). This servo mechanism results in agonist enhancement of barrier function by inhibiting leakage induced by pro-angiogenic stimuli, including VEGF and thrombin. Antagonism alone leads to barrier opening effects. These actions have been well documented in lung and skin vasculature, and having a matched agonist-antagonist pair

## MOL #49783

like CYM-5442 and W146 would be optimal for further studying the hypothetical endothelial S1P-S1P<sub>1</sub> rheostat.

Highly selective and potent chemical tools in general have characteristically slow off-rates, and have been of great interest in recent crystallographic studies (Cherezov et al., 2007; Rosenbaum et al., 2007) to define both orthosteric and spatially distinct hydrophobic binding pockets within this family of Class A GPCRs, and the minimalist changes in receptor structure necessary for full pharmacological efficacy. Such chemical tools, when deeply characterized and broadly available to the field (Rosen et al., 2008), can impact on the progress of mechanistic understanding in physiology, pathology and structural biology and ultimately on therapeutics.

### Acknowledgments

The authors are grateful to Bill Webb (Ctr. for Mass Spectrometry, TSRI) for measuring serum drug levels and Aaron Semana for expert technical assistance.

## References

- Ahmad M, Long JS, Pyne NJ and Pyne S (2006) The effect of hypoxia on lipid phosphate receptor and sphingosine kinase expression and mitogen-activated protein kinase signaling in human pulmonary smooth muscle cells. *Prostaglandins Other Lipid Mediat.* **79**: 278-286.
- Alfonso C, McHeyzer-Williams MG and Rosen H (2006) CD69 down-modulation and inhibition of thymic egress by short and long-term selective chemical agonism of S1P1 receptors. *Eur J Immunol.* **36**:149-159.
- Balatoni B, Storch MK, Swoboda EM, Schönborn V, Koziel A, Lambrou GN, Hiestand PC, Weissert R and Foster CA (2007). FTY720 sustains and restores neuronal function in the DA rat model of MOG-induced experimental autoimmune encephalomyelitis. *Brain Res Bull.* **74**:307-316.
- Cherezov V, Rosenbaum DM, Hanson MA, Rasmussen SG, Thian FS, Kobilka TS, Choi HJ, Kuhn P, Weis WI, Kobilka BK and Stevens RC (2007) High-resolution crystal structure of an engineered human beta2-adrenergic G protein-coupled receptor. *Science.* 318:1258-1265.
- Dudek SM, Jacobson JR, Chiang ET, Birukov KG, Wang P, Zhan X and Garcia JG (2004) Pulmonary endothelial cell barrier enhancement by sphingosine 1-phosphate: roles for cortactin and myosin light chain kinase. *J Biol Chem.* **279**: 24692-24700.
- Foss FW Jr, Snyder AH, Davis MD, Rouse M, Okusa MD, Lynch KR and Macdonald TL (2007) Synthesis and biological evaluation of gamma-aminophosphonates as

MOL #49783

- potent, subtype-selective sphingosine 1-phosphate receptor agonists and antagonists. *Bioorg Med Chem*, **15**: 663-677.
- Foster CA, Mechtcheriakova D, Storch MK, Balatoni B, Howard LM, Bornancin F, Wlachos A, Sobanov J, Kinnunen A and Baumruker T (2008) FTY720 Rescue Therapy in the Dark Agouti Rat Model of Experimental Autoimmune Encephalomyelitis: Expression of Central Nervous System Genes and Reversal of Blood-Brain-Barrier Damage. *Brain Pathology*. **In Press**.
- Fujiwara Y, Osborne DA, Walker MD, Wang DA, Bautista DA, Liliom K, Van Brocklyn JR, Parrill AL and Tigyi G (2007) Identification of the hydrophobic ligand binding pocket of the S1P<sub>1</sub> receptor. *J Biol Chem*. 282:2374-2385.
- Gonzalez-Cabrera PJ, Hla T and Rosen H (2007) Mapping Pathways Downstream of Sphingosine 1-Phosphate Subtype 1 by Differential Chemical Perturbation and Proteomics. *J Biol Chem*. **282**: 7254-7264.
- Hiestand PC, Rausch M, Meier DP and Foster CA (2008) Ascomycete derivative to MS therapeutic: S1P receptor modulator FTY720. *Prog Drug Res*. 66: 363-81.
- Jo E, Sanna MG, Gonzalez-Cabrera PJ, Thangada S, Tigyi G, Osborne DA, Hla T, Parrill AL and Rosen H (2005) S1P<sub>1</sub>-Selective In Vivo-Active Agonists from High-Throughput Screening: Off-the-Shelf Chemical Probes of Receptor Interactions, Signaling, and Fate. *Chem Biol*. **12**: 703-715.
- Kataoka H, Sugahara K, Shimano K, Teshima K, Koyama M, Fukunari A and Chiba K (2005) FTY720, sphingosine 1-phosphate receptor modulator, ameliorates experimental autoimmune encephalomyelitis by inhibition of T cell infiltration. *Cell Mol Immunol*. 2:439-448.

MOL #49783

- Lee M-J, Thangada S, Claffey KP, Ancellin N, Liu CH, Kluk M, Volpi M, Sha'afi RI, and Hla T (1999) Vascular endothelial cell adherens junction assembly and morphogenesis induced by sphingosine-1-phosphate. *Cell*. **99**: 301-312.
- Liu CH, Thangada S, Lee MJ, Van Brocklyn JR, Spiegel S, Hla T (1999) Ligand-induced trafficking of the sphingosine-1-phosphate receptor EDG-1. *Mol Biol Cell*. **10**: 1179-1190.
- Li Z; Chen W; Hale J; Lynch C L; Mills SG; Hajdu R; Keohane CA; Rosenbach MJ; Milligan JA; Shei G, Chrebet G; Parent SA, Bergstrom J, Card D, Forrest M, Quackenbush EJ, Wickham LA, Vargas H, Evans RM, Rosen H and Mandala S (2005) Discovery of potent 3,5-diphenyl-1,2,4-oxadiazole sphingosine-1-phosphate-1 (S1P1) receptor agonists with exceptional selectivity against S1P2 and S1P3. *J Med Chem*. **48**: 6169-6173.
- Mandala S, Hajdu R, Bergstrom J, Quackenbush E, Xie J, Milligan J, Thornton R, Shei GJ, Card D, Keohane C, Rosenbach M, Hale J, Lynch CL, Rupprecht K, Parsons W and Rosen H (2002) Alteration of lymphocyte trafficking by sphingosine-1-phosphate receptor agonists. *Science*. **296**: 346-349.
- Miron VE, Schubart A and Antel JP (2008) Central nervous system-directed effects of FTY720 (fingolimod) *J Neurol Sci*. **In press**
- Matloubian M, Lo CG, Cinamon G, Lesneski MJ, Xu Y, Brinkmann V, Allende ML, Proia RL and Cyster JG (2004). Lymphocyte egress from thymus and peripheral lymphoid organs is dependent on S1P receptor 1. *Nature*. **427**:355-360.
- Oo ML, Thangada S, Wu MT, Liu CH, Macdonald TL, Lynch KR, Lin CY and Hla T (2007) Immunosuppressive and anti-angiogenic sphingosine 1-phosphate

MOL #49783

- receptor-1 agonists induce ubiquitinylation and proteasomal degradation of the receptor. *J Biol Chem.* **282**: 9082-9089.
- Parrill AL, Wang D, Bautista DL, Van Brocklyn JR, Lorincz Z, Fischer DJ, Baker DL, Liliom K, Spiegel S and Tigyi G (2000). Identification of Edg1 receptor residues that recognize sphingosine 1-phosphate. *J Biol Chem.* **275**: 39379-39384.
- Rosen H, Alfonso C, Surh CD and McHeyzer-Williams MG (2003) Rapid induction of medullary thymocyte phenotypic maturation and egress inhibition by nanomolar sphingosine 1-phosphate receptor agonist. *Proc. Natl. Acad. Sci.* **100**: 10907-10912.
- Rosen H and Goetzl EJ (2005) Sphingosine 1-phosphate and its receptors: An autocrine and paracrine network. *Nat. Rev. Immunol.* **5**: 560-570.
- Rosen H, Sanna MG, Cahalan SM and Gonzalez-Cabrera PJ (2007) Tipping the gatekeeper: S1P regulation of endothelial barrier function. *Trends Immunol.* **28**: 102-107.
- Rosen H, Gonzalez-Cabrera PJ, Marsolais D, Cahalan SM, Don A and Sanna MG (2008) Modulating tone: the overture of S1P receptor immunotherapeutics. *Immunol. Rev.* **223**: 221-35.
- Rosenbaum DM, Cherezov V, Hanson MA, Rasmussen SG, Thian FS, Kobilka TS, Choi HJ, Yao XJ, Weis WI, Stevens RC and Kobilka BK (2007) GPCR engineering yields high-resolution structural insights into beta2-adrenergic receptor function. *Science.* **318**:1266-1273.
- Sanna MG, Liao J, Jo E, Alfonso C, Ahn MY, Peterson MS, Webb B, Lefebvre S, Chun J, Gray N and Rosen H (2004) Sphingosine 1-phosphate (S1P) Receptor Subtypes

MOL #49783

S1P1 and S1P3, Respectively, Regulate Lymphocyte Recirculation and Heart Rate. *J Biol Chem.* **279**: 13839-13848.

Sanna MG, Wang SK, Gonzalez-Cabrera PJ, Don A, Marsolais D, Matheu MP, Wei SH, Parker I, Jo E, Cheng WC, Cahalan MD, Wong CH and Rosen H (2006) Enhancement of capillary leakage and restoration of lymphocyte egress by a chiral S1P1 antagonist in vivo. *Nat Chem Biol.* **2**: 434-441.

Sanchez T, Estrada-Hernandez T, Paik JH, Wu MT, Venkataraman K, Brinkmann V, Claffey K and Hla T (2003) Phosphorylation and action of the immunomodulator FTY720 inhibits vascular endothelial cell growth factor-induced vascular permeability. *J Biol Chem.* **278**: 47281-47290.

Schurer SC, Brown SJ, Gonzalez-Cabrera PJ, Schaeffer M-T, Chapman J, Jo E, Chase P, Spicer T, Hodder P and Rosen H (2008) Ligand-Binding Pocket Shape Differences between Sphingosine 1-Phosphate (S1P) Receptors S1P1 and S1P3 Determine Efficiency of Chemical Probe Identification by Ultrahigh-Throughput Screening. *ACS Chem Biol.* **3**: 486-98.

Schwab SR and Cyster JG (2007) Finding a way out: lymphocyte egress from lymphoid organs. *Nat Immunol.* **8**: 1295-1301.

Sorensen SD, Nicole O, Peavy RD, Montoya LM, Lee CJ, Murphy TJ, Traynelis SF and Hepler JR (2003) Common signaling pathways link activation of murine PAR-1, LPA, and S1P receptors to proliferation of astrocytes. *Mol Pharmacol.* **64**:1199-209

Wang DA, Lorincz Z, Bautista DL, Liliom K, Tigyi G and Parrill AL (2001) A single amino acid determines lysophospholipid specificity of the S1P1 (EDG1) and

MOL #49783

LPA1 (EDG2) phospholipid growth factor receptors. *J Biol Chem.* 276:49213-49220.

Wei SH, Rosen H, Matheu MP, Sanna MG, Wang SK, Jo E, Wong CH, Parker I and Cahalan MD (2005) Sphingosine 1-phosphate type 1 receptor agonism inhibits transendothelial migration of medullary T cells to lymphatic sinuses. *Nat Immunol*, **6**: 1228-1235.

Yan L, Huo P, Doherty G, Toth L, Hale JJ, Mills SG, Hajdu R, Keohane C, Rosenbach MJ, Milligan MA, Shei G, Chrebet G, Bergstrom J, Card D, Quackenbush E, Wickham A and Mandala SM (2006) Discovery of 3-arylpropionic acids as potent agonists of sphingosine-1-phosphate receptor-1 (S1P<sub>1</sub>) with high selectivity against all other known S1P receptor subtypes. *Bioorg Med Chem Lett.* 16:3679-3683.

Yoon CM, Hong BS, Moon HG, Lim S, Suh PG, Kim YK, Chae CB and Ghoo YS (2008) Sphingosine-1-phosphate promotes lymphangiogenesis by stimulating S1P1/Gi/PLC/Ca<sup>2+</sup> signaling pathways. *Blood*. **In press**.



MOL #49783

## Footnotes

<sup>†</sup>:These authors equally contributed to the work.

Supported by National Institutes of Health grants AI-055509, MH-074404 and AI-074564).

MOL #49783

## Figure legends

**Figure 1.** Chemical structure of ligands used in this study.

**Figure 2.** Chemical synthesis of CYM-5442.

**Figure 3. Concentration dependent inhibition of CRE transcription in stable S1P<sub>1</sub>.CHO cells by S1P<sub>1</sub> agonists.** Cells stably expressing a CRE-beta-lactamase reporter and human S1P<sub>1</sub> were incubated with increasing concentrations of SEW2871, CYM-5442 or CYM5181. The ability of the agonists to inhibit forskolin-stimulated beta-lactamase expression was measured as described (Schurrer *et al.*, 2008). The potency (pEC<sub>50</sub>) values were determined to be -7.54, -8.47 and -8.91 for SEW2871, CYM5181 and CYM-5442, respectively.

**Figure 4. CYM-5442 activates three S1P<sub>1</sub> dependent pathways in stable S1P<sub>1</sub>-GFP 293 cells.** The ability of CYM-5442 to stimulate S1P<sub>1</sub> phosphorylation, S1P<sub>1</sub> internalization and S1P<sub>1</sub> ubiquitylation was measured in HEK293 cells expressing human S1P<sub>1</sub> tagged to C-terminal GFP. **(A)** Time-dependent induction of S1P<sub>1</sub> phosphorylation by CYM-5442 is abolished by the S1P<sub>1</sub> antagonist W146. Orthophosphate-P<sup>32</sup> labeled cells were incubated with CYM-5442 for the indicated times, followed by S1P<sub>1</sub> immunoprecipitation using GFP. Immunoprecipitates were then run by SDS-PAGE, and exposed to determine whole receptor phosphorylation status. The silver stained gel (bottom panel) confirmed equal loading of immunoprecipitated S1P<sub>1</sub>-GFP across

MOL #49783

conditions. The mass ladder is indicated in KDa. **(B)** CYM-5442 stimulates internalization of S1P<sub>1</sub>-GFP from the plasma membrane into cytoplasmic vesicles (at 45 min incubation, middle panel), while W146 preincubation (30 min, lower panel) blocks CYM-5442-mediated internalization. W146 alone had no effect on internalization (upper panel). Representative micrographs are shown (n=3); 20  $\mu$ m scale bar; 40X. **(C)** CYM-5442 induces S1P<sub>1</sub> ubiquitylation (UB-S1P<sub>1</sub>-GFP) by similar magnitude vs. the full, non-selective S1P receptor agonist, AFD-R (top immunoblot). Note that CYM-5442 ubiquitylation is abolished by W146 preincubation. For this experiment, AFD-R and CYM-5442 were incubated for 1 h and W146 was included 30 min prior to CYM-5442 stimulation. Equal loading of immunoprecipitated S1P<sub>1</sub> receptor was confirmed by reblotting for GFP (bottom immunoblot). The mass ladder is indicated in KDa. This experiment was repeated twice with similar results.

**Figure 5. CYM-5442 does not require two essential S1P headgroup receptor interactions for activating p42/p44 MAPK.** Wild-type (WT) human S1P<sub>1</sub> and two single-point S1P<sub>1</sub> receptor mutants (R<sup>120</sup>A and E<sup>121</sup>A), reported to independently disrupt S1P-S1P<sub>1</sub> binding and/or S1P-S1P<sub>1</sub> function, were transiently transfected into CHO-K1 cells. Following 48 h, cells were stimulated for 5 min with increasing concentrations of S1P or CYM-5442, and agonist-dependent S1P<sub>1</sub> activation of p42/p44 MAPK activity was determined using ELISA studies. Parallel agonist concentration responses were also performed with cells that had been preincubated with 10  $\mu$ M of W146 for 30 min. For each of the three conditions, the fitted curves are the mean  $\pm$  SD of three independent experiments. The potency (pEC50), intrinsic activity (Emax) and goodness of fit (R<sup>2</sup>)

MOL #49783

derived from the agonists' activation curves were determined for WT, R<sup>120</sup>A and E<sup>121</sup>A transfected cells, both in the absence (-) or presence (+) of the S1P<sub>1</sub> antagonist W146. These values are shown in Table 1.

**Figure 6. CYM-5442 induction of lymphopenia in mice is dose- and time-dependent.**

C57BL/6J male mice (three mice for group) were injected i.p. with either increasing doses of CYM-5442 or vehicle (water) to determine the dose dependence of CYM-5442 for induction of lymphopenia, or with a fixed dose (10 mg/kg) of CYM-5442 or vehicle for time-course studies. For these studies, blood was extracted from each animal and used to measure B220<sup>+</sup>, CD4<sup>+</sup> and CD8<sup>+</sup> cell counts, as well as CYM-5442 serum concentration. (A) The average inhibition of single-positive CD4 (CD4<sup>+</sup>, red) and CD8 (CD8<sup>+</sup>, green) T-cell number is shown at the indicated dose of CYM-5442. The mean serum CYM-5442 concentration reveals that a 50-100 nM free CYM-5442 concentration range is required for induction of lymphopenia at 5 h. (B) Representative plots of B220<sup>+</sup> (blue), CD4<sup>+</sup> (red) and CD8<sup>+</sup> (green) percent decreases are shown at the indicated CYM-5442 dose. (C) The mean dose-response for CYM-5442 mediated inhibition of B220<sup>+</sup>, CD4<sup>+</sup> and CD8<sup>+</sup> cell counts was used to calculate the ED<sub>50</sub>s (D) Time-course of inhibition of CD4<sup>+</sup> and CD8<sup>+</sup> T-cell number following 10 mg/kg CYM-5442. The mean CYM-5442 serum concentration is also plotted. (E) Characteristic scatter plots of CYM-5442 percent inhibition of B-cell (B-220<sup>+</sup>, blue) and T-cell (CD4<sup>+</sup>, red and CD8<sup>+</sup>, green) numbers are shown following 1, 3, 5, 8 and 16 h post CYM-5442 administration.

MOL #49783

**Table 1. Selectivity of CYM-5442 for the cloned human S1P receptors.** In agonist format, CYM-5442 was tested in 12-point (up to 10  $\mu$ M) concentration response curves. In antagonist format, CYM-5442 was included in the assay at 10  $\mu$ M final concentration and tested for its potential to block an EC80 concentration of S1P.

Receptor subtype	Agonist format (Emax) (EC50)	Antagonist format (IC50)
S1P <sub>1</sub> <sup>a</sup>	(100%) (1.35 $\pm$ 0.25 nM)	N.A.
S1P <sub>2</sub> <sup>b</sup>	N.A.	N.A.
S1P <sub>3</sub> <sup>c</sup>	N.A.	N.A.
S1P <sub>4</sub> <sup>d</sup>	N.A.	N.D.
S1P <sub>5</sub> <sup>e</sup>	20% at 10 $\mu$ M	N.D.

N.A. refers to no activity; N.D., not determined

<sup>a</sup> Agonist format measured forskolin-stimulated CYM-5442 inhibition of cAMP CRE transcription on stable S1P<sub>1</sub>-CHO-K1-CRE-bla cells, with SEW2871 as positive control. W146 inhibition of SEW2871 was used as a positive control in the antagonist format

<sup>b</sup> Agonist format measured CYM-5442-stimulated cAMP accumulation on stable CHO-K1-S1P<sub>2</sub>-CRE cells with S1P as positive control. JTE-013 inhibition of S1P was used as positive control in antagonist format

<sup>c</sup> Agonist format measured CYM-5442-stimulated cAMP accumulation in stable S1P<sub>3</sub>-NFAT-bla-CHO-K1 cells with S1P as positive control.

<sup>d</sup> Agonist format measured CYM-5442-stimulated  $\beta$ -arrestin activation in stable TANGO<sup>®</sup> S1P<sub>4</sub>-bla U2OS cells with S1P as positive control.

<sup>e</sup> Agonist format measured CYM-5442-stimulated cAMP accumulation in stable TANGO<sup>®</sup> S1P<sub>5</sub>-bla U2OS cells with S1P as positive control.

MOL #49783

**Table 2. CYM-5442 does not require essential S1P headgroup-receptor interactions for activating p42/p44 MAPK.** Mean potency (EC<sub>50</sub>), intrinsic activity (E<sub>max</sub>) and goodness of fit (R<sup>2</sup>) values for the S1P and CYM-5442 response curves depicted in Figure 4. Minus (-) and plus (+) refer to the presence or absence of 10 μM W146 in the assay.

	WT				R <sup>120</sup> A				E <sup>121</sup> A			
	S1P		5442		S1P		5442		S1P		5442	
	-	+	-	+	-	+	-	+	-	+	-	+
<b>LogEC<sub>50</sub></b>	-8.6	-6.8	-7.3	-5.7	-7.2	-7.7	-7.2	-6.8	-6.8	-7.2	-6.9	-5.9
<b>E<sub>max</sub> (%)</b>	100	90	70	7	25	17	100	86	27	27	100	80
<b>R<sup>2</sup></b>	0.98	0.98	0.95	NF	NF	NF	0.98	0.99	NF	NF	0.99	0.79

NF: no fit

MOL #49783

**Table 3.** Pharmacokinetic parameters of CYM-5442 in rats.

Parameters	CYM-5442 (2 mg/kg; PO <sup>a</sup> )	CYM-5442 (1 mg/kg; i.v. <sup>a</sup> )
t <sub>1/2</sub>	4.00 ± 1.45	3.05 ± 0.37
MRT (h)	6.35 ± 2.10	3.54 ± 0.38
Cl (ml/min/kg)	360.1 ± 73.3	72.90 ± 11.70
V <sub>ss</sub> (L)	ND	15.60 ± 3.50
AUC (μM.h)	0.23 ± 0.053	0.57 ± 0.10
AUC (% extrap,ob)	27.80 ± 14.20	11.35 ± 14.20
C <sub>max</sub> (nM)	36 ± 7.2	220.0 ± 18.0
T <sub>max</sub>	1.17 ± 0.76	0.083 ± 0.00
F%	20.50 ± 4.67	ND

<sup>a</sup>Formulation (% v/v): 10/10/80 (DMSO/Tween-20/ water)

ND, not determined

MOL #49783

**Table 4. Acute CYM-5442 administration induces lymphopenia in mice.** Mice (three per group) were injected i.p. with a dose of 10 mg/kg in a 300 µl volume. Vehicle control mice received sterile water injections. Five hours post treatment, animals were euthanized and blood was collected into tubes containing EDTA. Blood lymphopenia was assessed by comparing absolute white blood cell (WBC) number between CYM-5442-treated and vehicle-treated animals, as measured with an automated hem analyzer. In addition, FACS analyses were used to measure blood B220-positive cells (B220<sup>+</sup>, a marker for B-cells), and from the B220<sup>+</sup> population, the percent of single-positive CD4 (CD4<sup>+</sup>) and CD8 (CD8<sup>+</sup>) T-cells.

Parameters	Vehicle	CYM-5442
WBC (K/mm <sup>3</sup> )	11.9±0.2	4.3±0.4*
% B220 <sup>+</sup>	40.5±0.6	14.7±0.5*
% CD4 <sup>+</sup>	11.5±0.2	1.9±0.2*
% CD8 <sup>+</sup>	11.9±0.3	1.9±0.4*

\*P<0.05 vs. vehicle treated



MOL #49783

**Table 5. Lymphopenia by CYM-5442 administration is S1P<sub>1</sub> dependent.** Mice

(three per group) were first injected i.p. with a 20 mg/kg W146 in a 300 µl volume.

W146 vehicle control mice received equal volume of 10 mM sodium carbonate: 2% β-cyclodextrin (vol/vol). Thirty minutes later, animals were injected with either 2 mg/kg CYM-5442 or vehicle (sterile water). Five hours post CYM-5442 treatment, animals were euthanized and blood was collected into tubes containing EDTA. The number of B220-positive cells (B220<sup>+</sup>, a marker for B-cells) and single-positive CD4 (CD4<sup>+</sup>) and CD8 (CD8<sup>+</sup>) T-cells were determined by FACS analysis and expressed as a percent change relative to values obtained in animals receiving both drug vehicles. A sample aliquot of the blood was used to measure the serum drug concentration levels by LC-MS/MS. Drug concentrations are included in parentheses in µM (± SD).

	<b>W146 alone</b> (1.75±0.56)	<b>CYM-5442</b> (0.18±0.05)	<b>W146 + CYM-5442</b> (1.76±0.31)(0.19±0.04)
<b>B220<sup>+</sup></b>	114.7±5.9	46.0±18.1*	92.4±31.2
<b>CD4<sup>+</sup></b>	108.1 ±17.4	53.5 ± 6.5*	89.1±18.7
<b>CD8<sup>+</sup></b>	112.2±19.6	47.4±7.5*	92.2±15.1

\*p<0.05 relative to W146 alone

# Sphingosine 1-phosphate

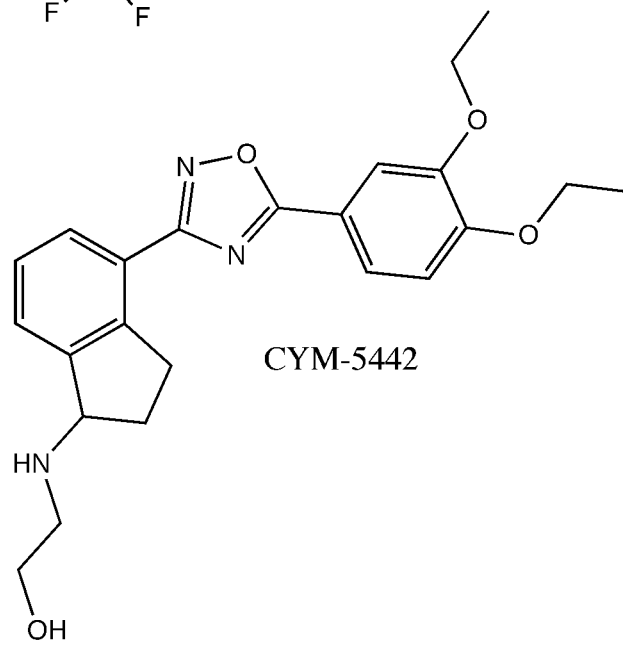
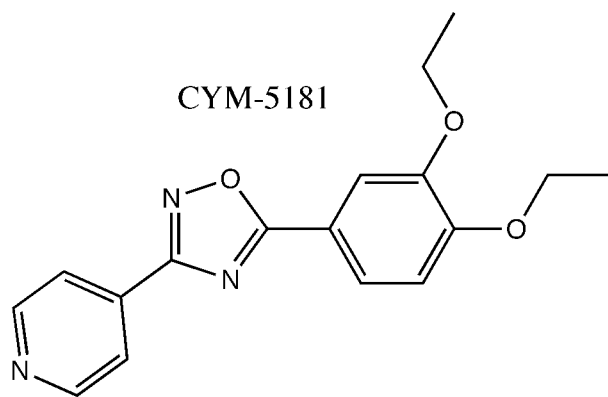
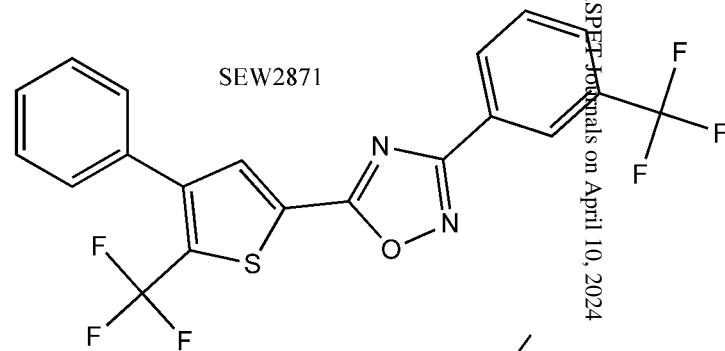
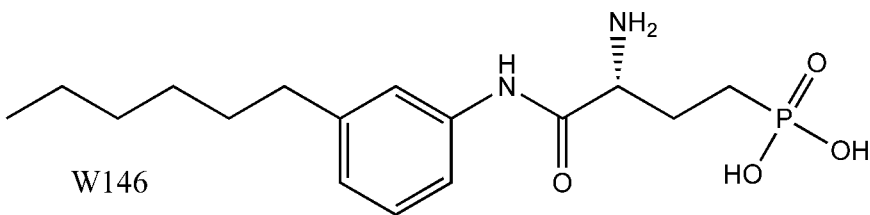
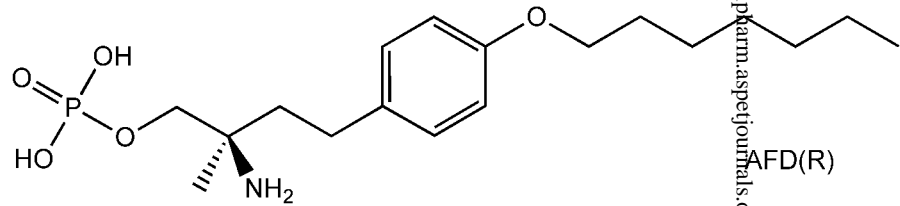
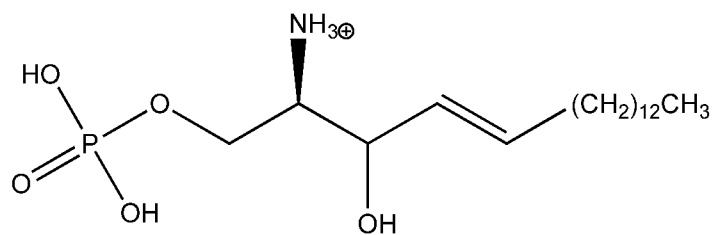
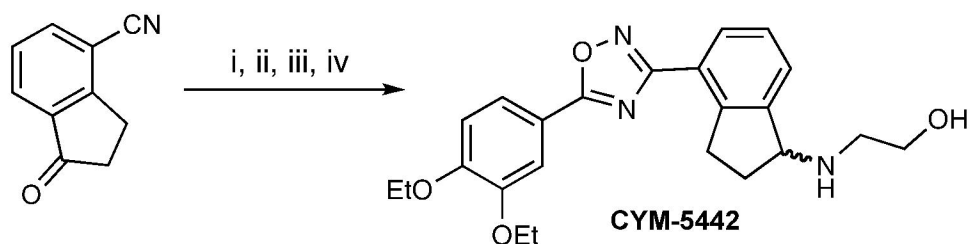


Figure 2



i.-  $\text{NaBH}_4$ ,  $\text{SiO}_2$ , EtOH, 0 °C to r.t., 2h. ii.-  $\text{NH}_2\text{OH}\cdot\text{HCl}$ ,  $\text{Na}_2\text{CO}_3$ , EtOH, reflux, 12h.  
iii.- 3,4-diethoxybenzoic acid, EDCI, HOBT, DMF, 130 °C, m.w., 30min. iv.- (a)  $\text{SOCl}_2$ , Py, r.t., 2h. (b) Aminoethanol, DIPEA, DMF, 50 °C, 48h.

Figure 3

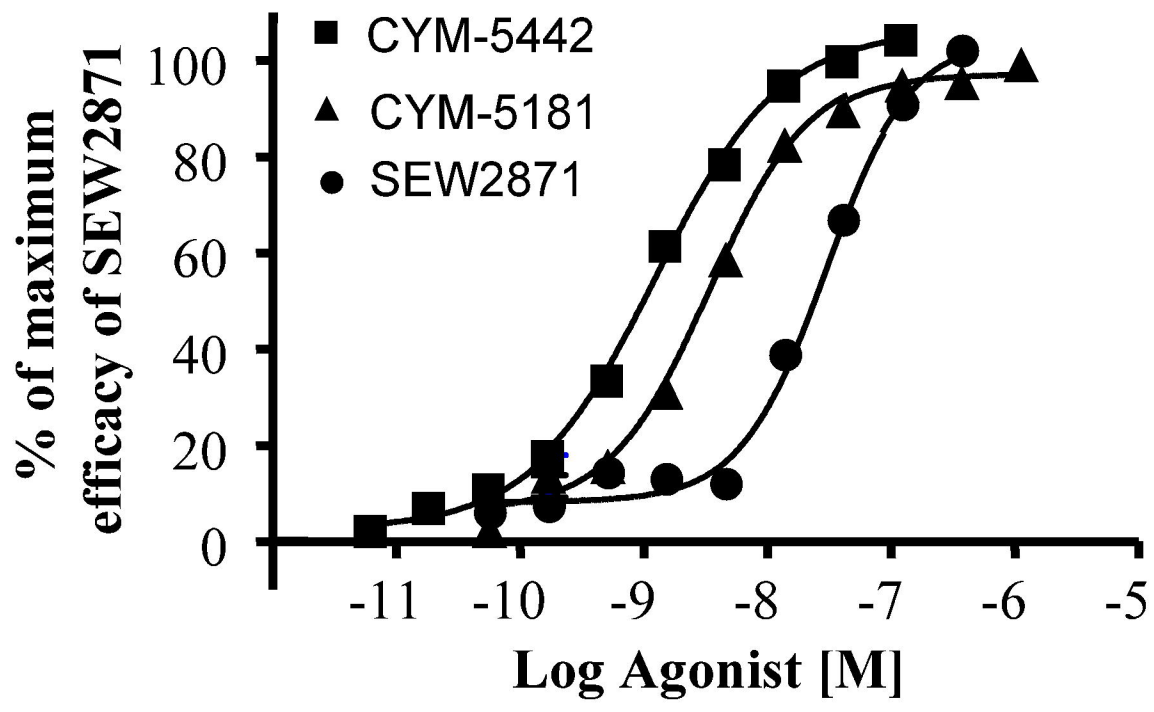
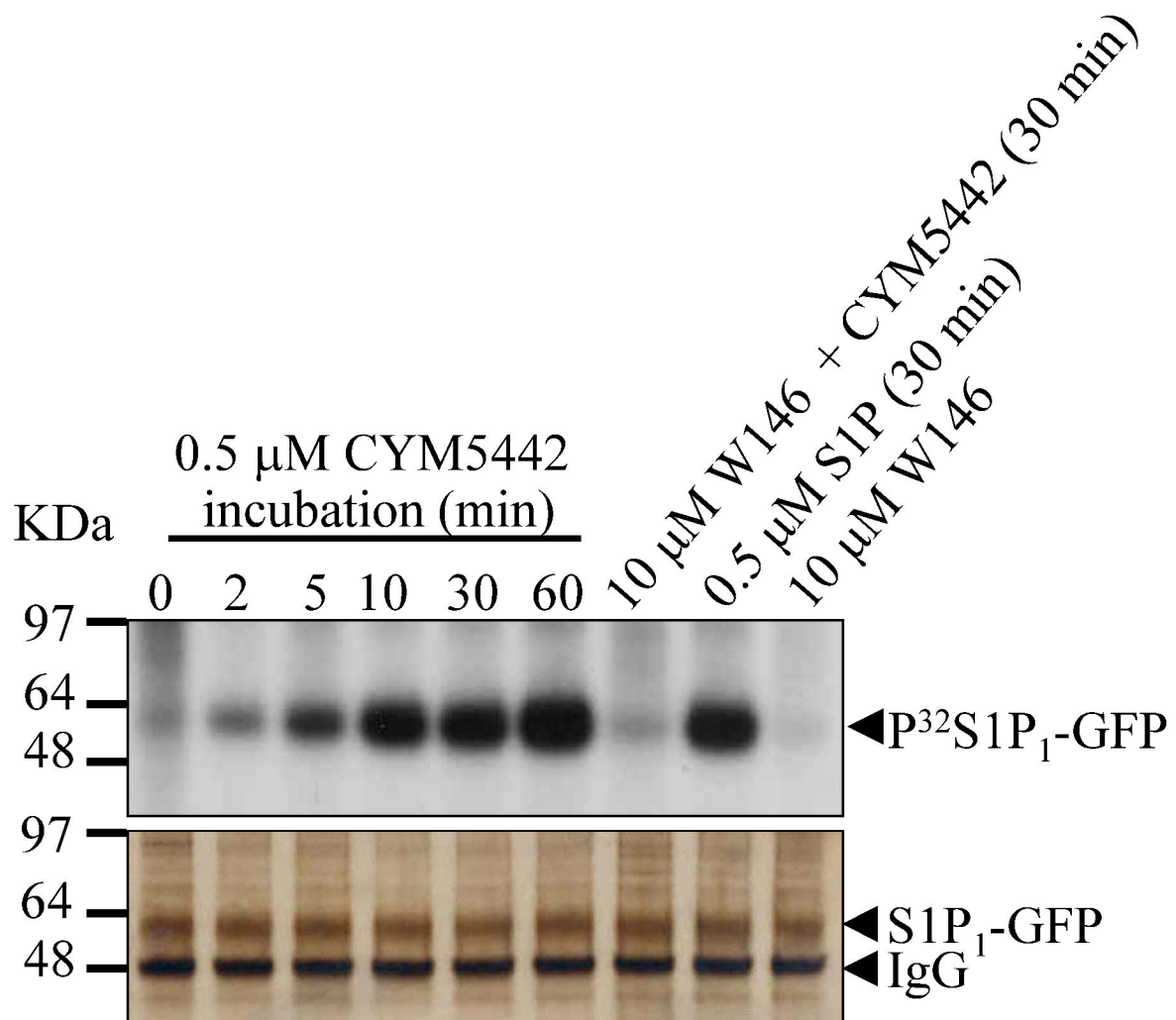
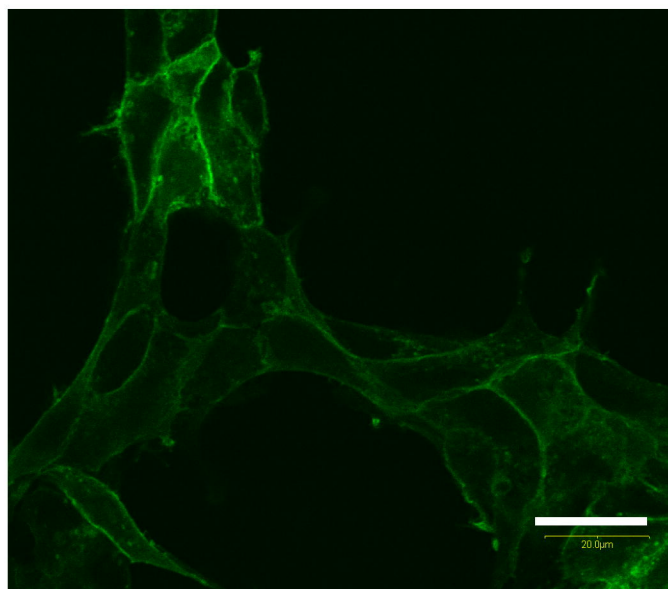


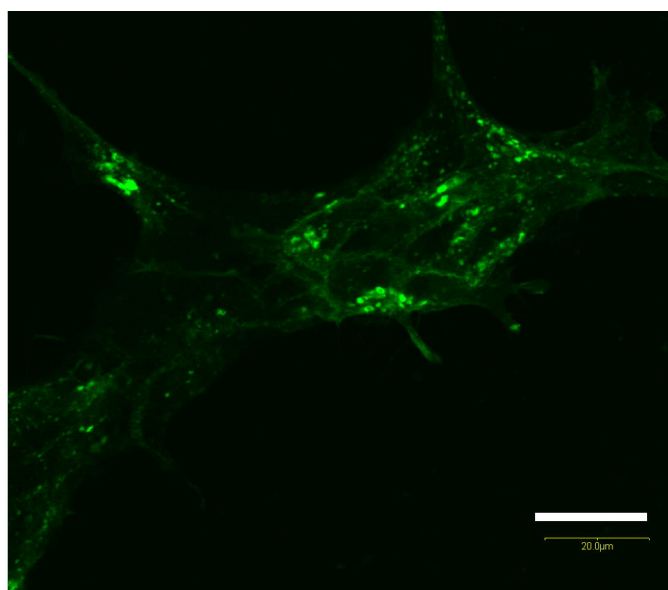
Figure 4A



**10  $\mu$ M W146**



**0.5  $\mu$ M CYM-5442**



**10  $\mu$ M W146 +  
0.5  $\mu$ M CYM-5442**

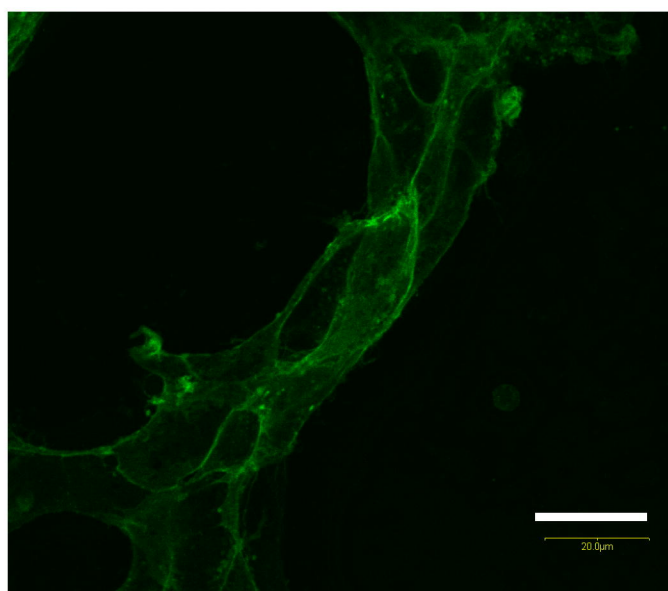


Figure 4C

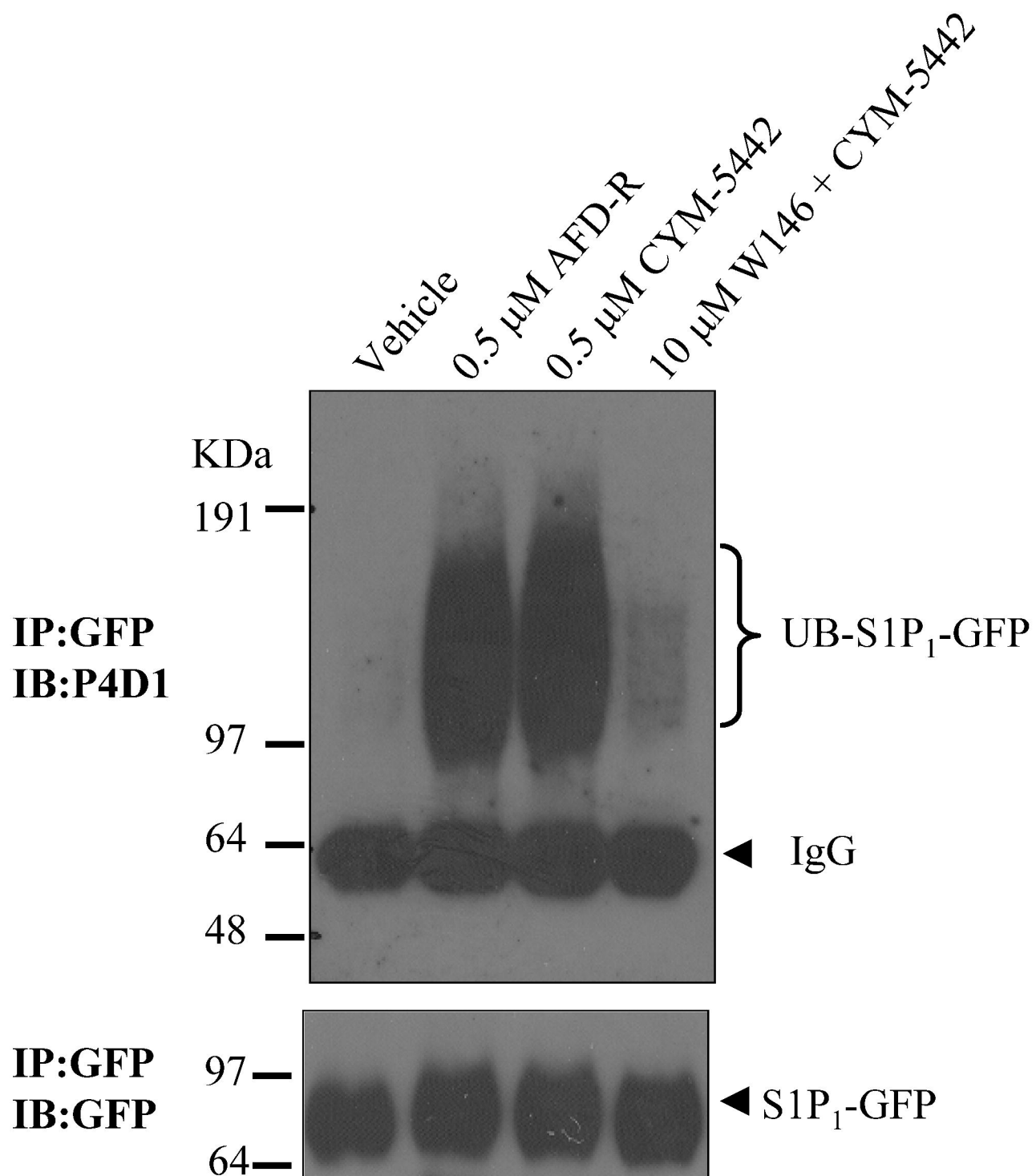
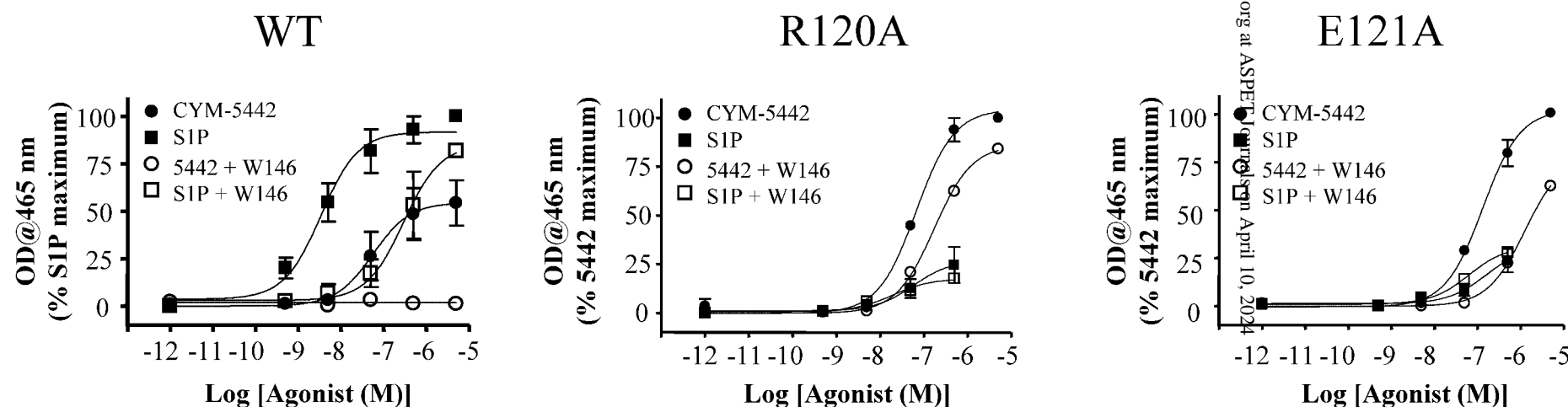


Figure 5



Downloaded from molpharm.aspetjournals.org at ASPET Journals on April 10, 2024



Figure 6A

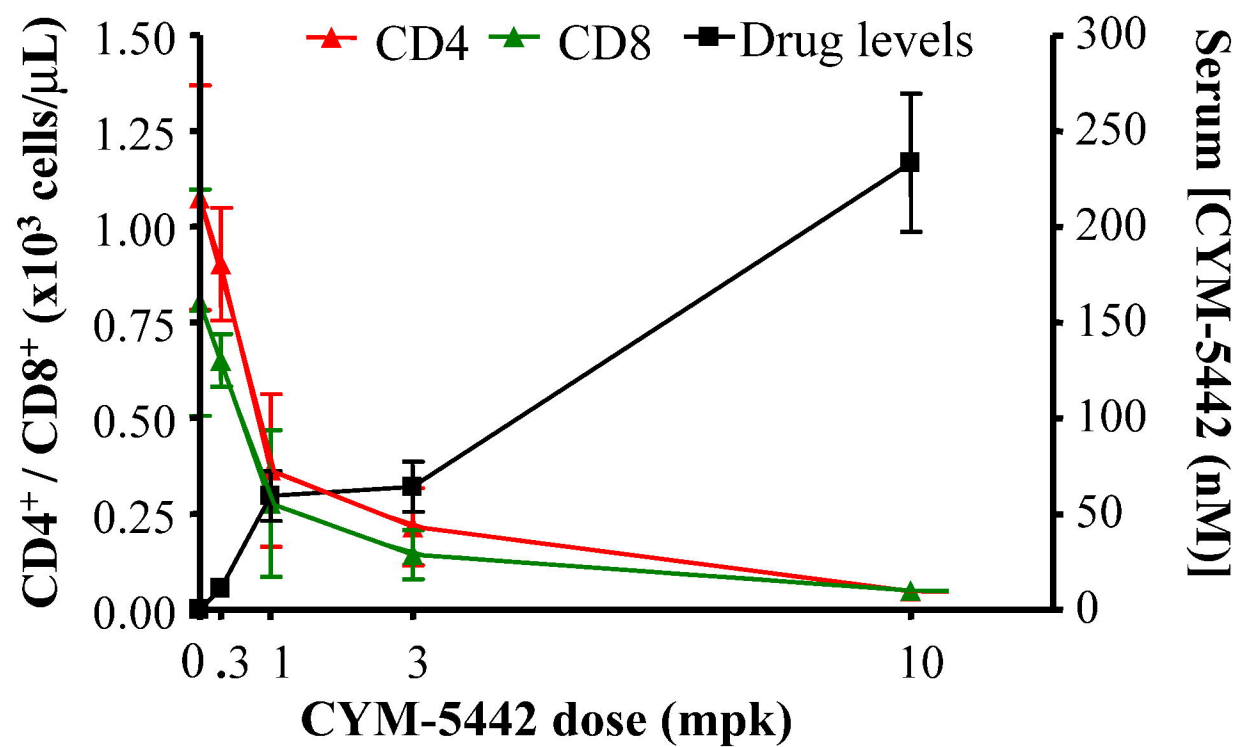


Figure 6B

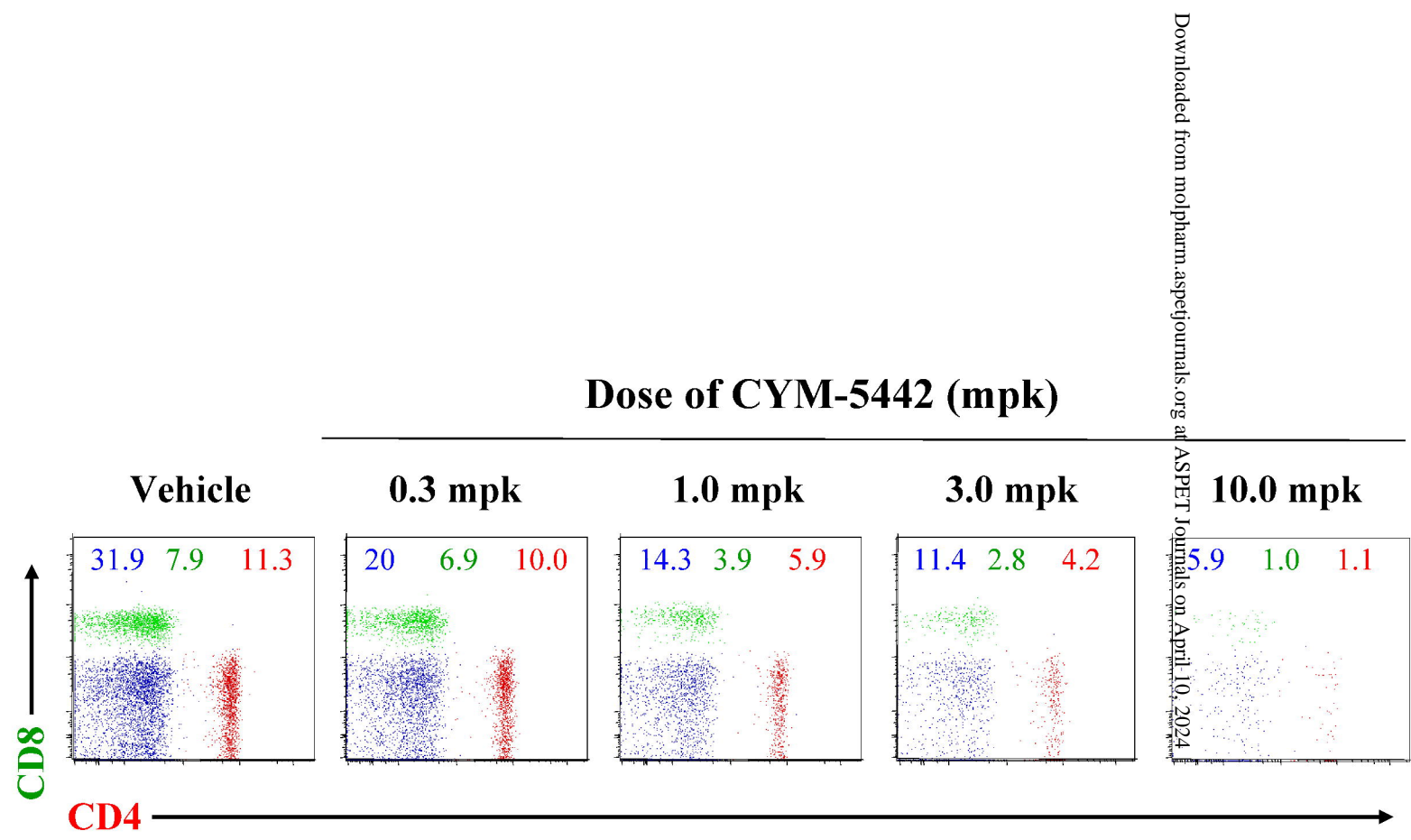
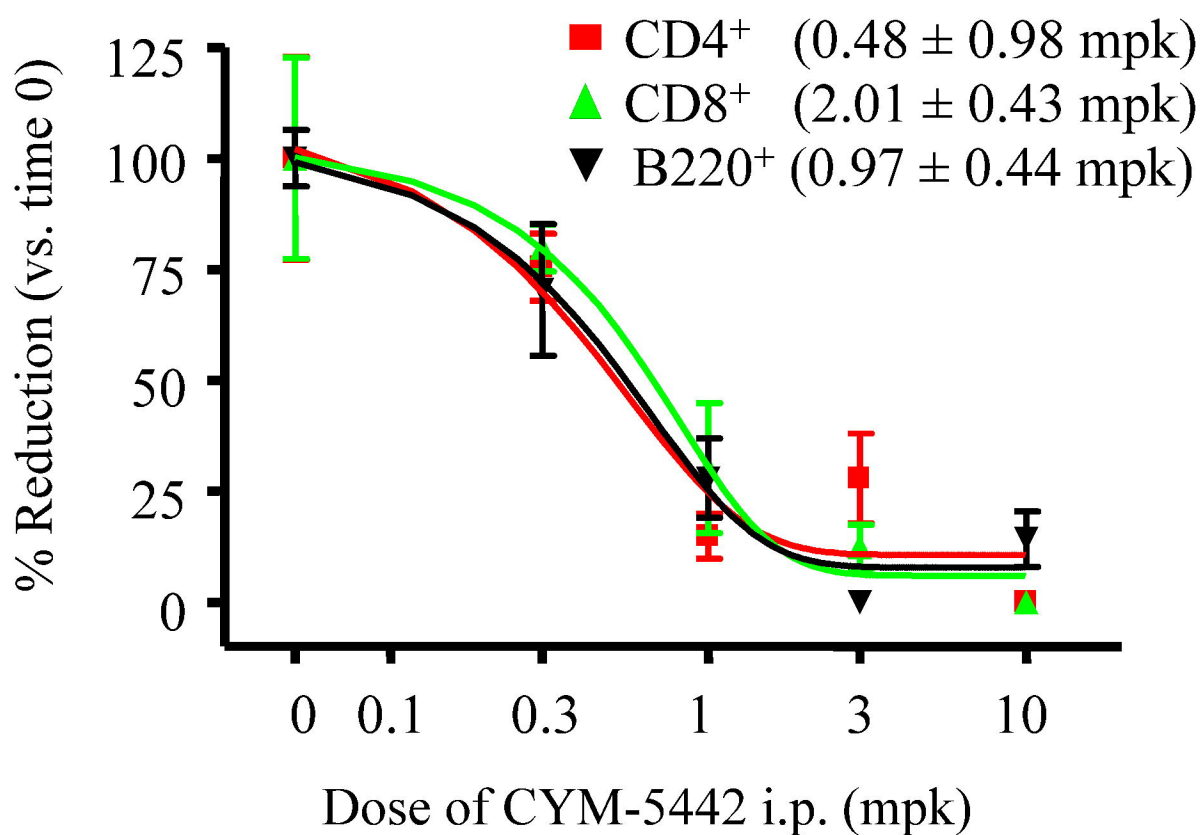


Figure 6C



**Figure 6D**

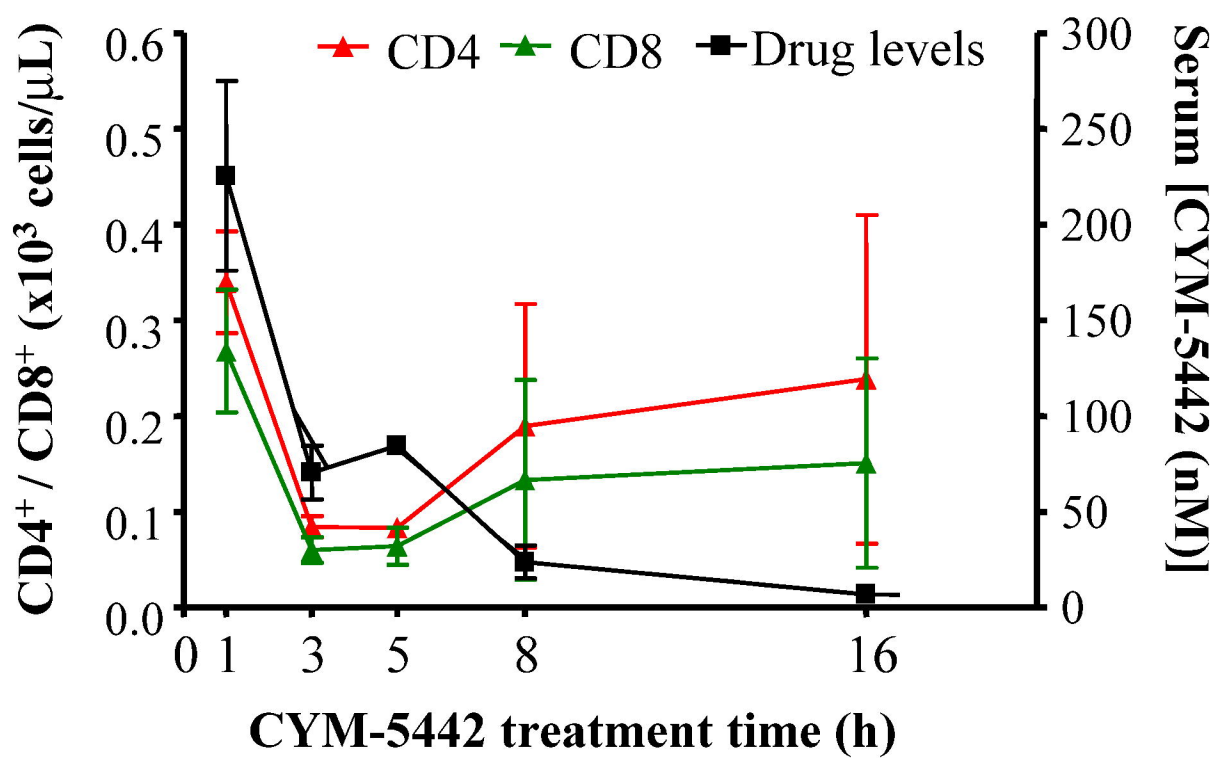


Figure 6E

